NRC Research Press

ARTICLE

Temporal and spatial evolution of Northern Cascade Arc magmatism revealed by LA–ICP–MS U–Pb zircon dating

Emily K. Mullen, Jean-Louis Paquette, Jeffrey H. Tepper, and I. Stewart McCallum

Abstract: We present thirty new laser ablation inductively coupled plasma mass spectrometry U–Pb zircon dates for intermediate to silicic plutons of the Northern Cascade Arc with emphasis on the Chilliwack batholith – Mount Baker magmatic focus, located in southwestern British Columbia and northern Washington. Chilliwack magmatism commenced at ~35 Ma in southwestern British Columbia and the most voluminous plutons define a cluster at ~32–29 Ma, documenting an early flare-up. During the same interval, the Index, Squire Creek, and Cascade Pass intrusions were emplaced south of the Chilliwack batholith. North of the Chilliwack, maximum pluton ages become progressively younger northward, tracking the northerly migration of the edge of the Farallon–Juan de Fuca–Explorer plate system relative to North America. Chilliwack magmatism continued from ~29 Ma to 22 Ma at a slightly reduced flux, followed by a lull from 22 to 11 Ma during which magmatism shifted north to the Mount Barr batholith (18 Ma). Chilliwack magmatism resumed by 11 Ma but was intermittent and the intrusive flux was significantly lower. The temporal decrease in intrusive flux displayed by the Chilliwack batholith correlates with the declining convergence rate of the Juan de Fuca plate since arc inception. The 11 Ma-to-present magmatism extends a pattern of southwesterly migration of the magmatic focus previously identified from ~4 Ma (Hannegan caldera) to the modern Mount Baker volcanic field. Crustal rotation accounts for the rate of the first ~7 million years of migration. However, the migration rate more than doubled at ~4 Ma, coinciding with separation of the Explorer plate and initiation of Juan de Fuca plate rollback.

Résumé : Nous présentons trente nouvelles datations U–Pb sur zircons par LA–ICP–MS de plutons acides à intermédiaires du nord de l'arc des Cascades, principalement de l'ensemble du batholithe de Chilliwack – mont Baker (sud-ouest de la Colombie-Britannique et nord de l'État de Washington). Ce magmatisme débute vers 35 Ma dans le sud-ouest de la Colombie-Britannique, et les plutons les plus volumineux définissent un pic d'activité précoce de ~32 Ma à ~29 Ma. Durant cette période, les intrusions d'Index, de Squire Creek et de Cascade Pass se mettent en place au sud du batholithe de Chilliwack. Dans la partie septentrionale, les âges maximums des plutons diminuent progressivement vers le nord, suivant la migration du système des plaques Farallon–Juan de Fuca–Explorer par rapport à l'Amérique du Nord. Un flux magmatique réduit se poursuit de ~29 Ma à 22 Ma, suivi d'une pause de 22 Ma à 11 Ma au cours de laquelle le magmatisme se déplace vers le nord (batholithe du mont Barr, 18 Ma). Un magmatisme intermittent de moindre intensité reprend à partir de 11 Ma. Cette baisse d'intensité est corrélée à une décélération de la convergence de la plaque Juan de Fuca. Le magmatisme de 11 Ma au présent prolonge la migration vers le sud-ouest à partir de ~4 Ma (caldera d'Hannegan) déjà décrite vers l'actuel domaine volcanique du mont Baker. Une rotation crustale explique la vitesse de migration durant les premières ~7 M années, qui double vers 4 Ma, au moment de la séparation de la plaque Explorer et le début du recul de la plaque Juan de Fuca. [Traduit par la Rédaction]

Introduction

A growing number of studies in exhumed paleo-arc systems have documented the episodic nature of arc magmatism through space and time (e.g., Paterson and Ducea 2015; Kirsch et al. 2016), with important implications for our understanding of the assembly and evolution of arcs and role of tectonic processes. A key element in these investigations has been the ability to determine high-quality crystallization ages on magmatic rocks. With exposures of some of the youngest arc plutons in the world, the Cascade Arc of western North America (Fig. 1) offers an opportunity to examine the temporal and spatial evolution of magmatism in a still-active arc. Recent comprehensive, high-precision $^{40}Ar/^{39}Ar$ and K–Ar dating studies have established chronologies for many of the active Cascade volcanic fields (e.g., Hildreth and Lanphere 1994; Hildreth et al. 2003; Bacon and Lanphere 2006; Clynne et al. 2008; Schmidt and Grunder 2009; Muffler et al. 2011; Fleck et al. 2014; Hildreth and Fierstein 2015), and several studies have sought to define the evolution of magma compositions and production rates in the Central and Southern Cascades (McBirney 1978; Verplanck and Duncan 1987; Priest 1990; Sherrod and Smith 2000; du Bray and John 2011; du Bray et al. 2014). However, these studies did not include a major segment of the arc, the Northern Cascades (here defined as that part of the arc north of Mount Rainier) of Washington and British Columbia, which offers the best exposures of the plutonic roots of the arc due to rapid Pleistocene uplift and extensive glacial erosion. Most of the existing radiometric dates for the early products of the Cascade Arc were also measured by old and relatively imprecise K–Ar or zircon fission track dating, with uncertainties in the millions of years. As a consequence, the timing of arc initiation as a function of position along

Received 27 July 2017. Accepted 24 January 2018.

Paper handled by Associate Editor Christopher McFarlane.

E.K. Mullen and J.-L. Paquette. Laboratoire Magmas et Volcans, Université Clermont Auvergne, 63178 Aubière, France.
J.H. Tepper. University of Puget Sound, Geology Department, Tacoma, WA 98416-1048, USA.
I.S. McCallum. University of Washington, Department of Earth and Space Sciences, Seattle, WA 98195-1310, USA.
Corresponding author: Emily K. Mullen (email: mullen.emka@gmail.com).

Fig. 1. (*a*) Geological elements of the Cascade Arc. The area in the gray box is enlarged in (*b*). (*b*) Map showing location of magmatic rocks in the Northern Cascade Arc (Mount Rainier to the north). The area enclosed by the red box (the Chilliwack–Mount Baker magmatic focus) is shown on an expanded scale in Fig. 2. Juan de Fuca and Gorda plate configurations are from McCrory et al. (2014); Explorer plate from Rohr and Tryon (2010) and Rohr (2015). [Colour online.]

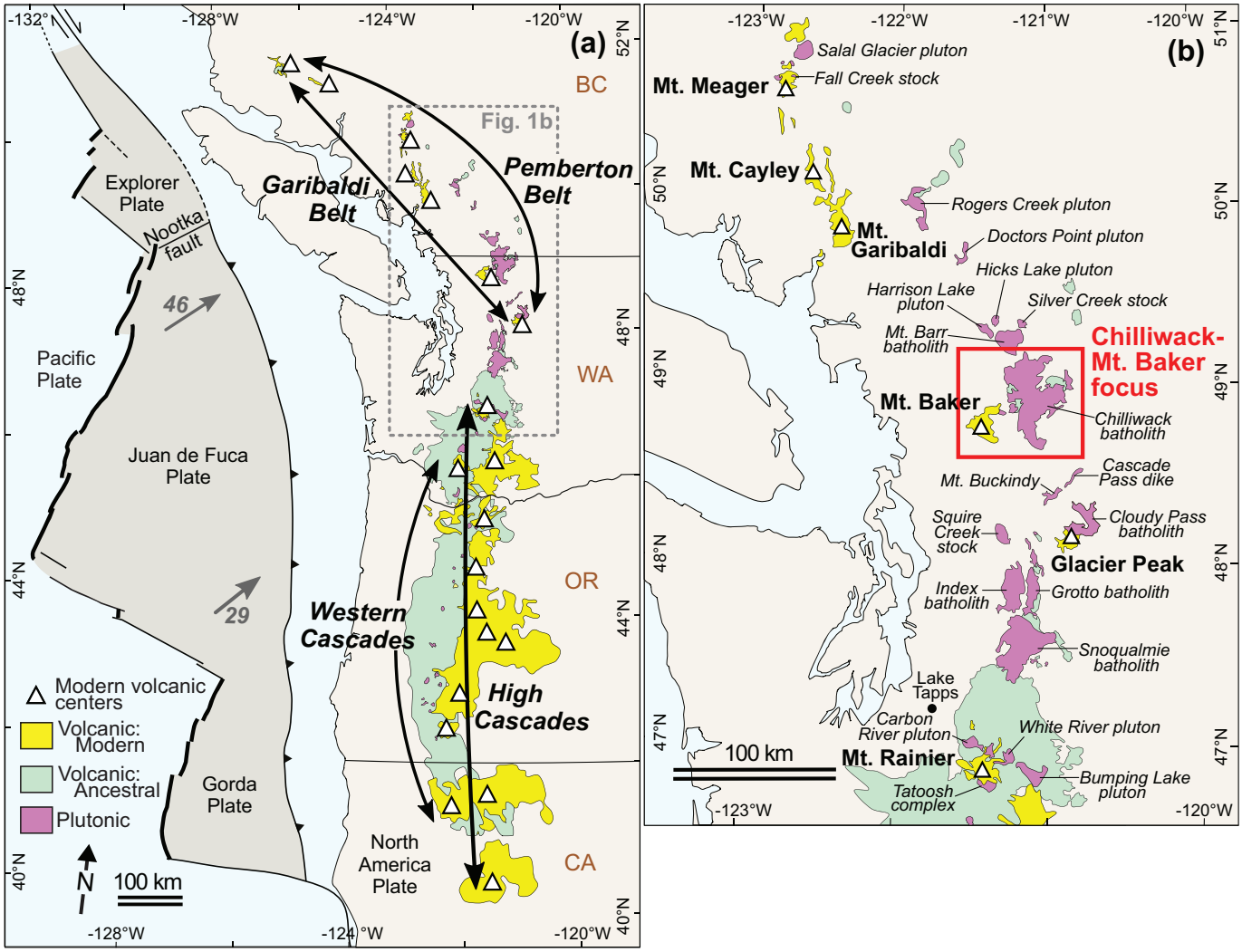

the arc axis and the evolution of the distribution and volumes of magmatism through time are incompletely known.

This study presents new U–Pb zircon ages for ancestral magmas of the Northern Cascade Arc, measured by laser ablation (LA) – inductively coupled plasma (ICP) – mass spectrometry (MS), to refine the spatial and temporal evolution of this sector of the arc. LA–ICP–MS is an ideal method for dating such relatively young samples because analytical uncertainties of less than 1% can be achieved at the 2σ level, which translates to tens or a few hundreds of thousands of years, shorter than the timescales of the magmatic processes of interest. This technique also affords the high spatial resolution needed to identify inherited zircons and multiple age domains within individual grains as well as the ability to rapidly produce large datasets. We primarily examine the ~960 km² composite Chilliwack batholith of northern Washington and southern British Columbia and its successor, the currently active Mount Baker volcanic field, which together preserve one of the longest and most continuously exposed magmatic records in the Cascades (Figs. 1, 2). In addition to 19 new dates for the area comprising the Chilliwack–Mount Baker magmatic focus (as defined in Figs. 1 and 2), we have determined ages for six arc plutons north of the Chilliwack batholith (Pemberton Belt; Fig. 1) and five samples from intrusions south of the batholith. Our goals are to improve the knowledge of Northern Cascades magmatic chronologies, to determine how magma fluxes and distributions have changed spatially and temporally, and to evaluate the contributing roles of forcing factors both internal and external to the arc, such as tectonic processes and the structure and characteristics of the mantle and crust of the arc system (Paterson and Ducea 2015).

Geological context

The Cascade Arc system

The Cascade Arc currently extends from northern California to southwestern British Columbia and is related to the northeasterly subduction of the Juan de Fuca oceanic plate (Fig. 1), a remnant of the once considerably larger Farallon plate (e.g., Schellart et al. 2010). Cascadia subduction was initiated after a westward trench jump following the accretion of the Siletz terrane, a process that was essentially complete by 45 Ma, although related basaltic volcanism of the Coast Range persisted through the earliest Cascade Arc magmatism (Wells et al. 2014). The oldest radiometrically measured dates for magmatic products of the Cascade Arc cluster at ~35–40 Ma with a few outlying points of up to ~42 Ma (Lux 1981; Sherrod and Smith 2000; du Bray and John 2011). Over time,

Fig. 2. Map of the Chilliwack–Mount Baker magmatic focus, based on the maps of Tabor et al. (2003), Hildreth et al. (2003), Monger (1989), Richards and McTaggart (1976), and Tepper (1991). Magmatic rocks older than 1 Ma are color-coded in three phases based on the new dates, augmented by dates from previous studies (Tabor et al. 2003 and references therein). Note that the sample dated from the Kulshan caldera was collected farther south near Lake Tapps, as discussed in the main text (Fig. 1*b*). The 31.95 Ma Hannegan Trail unit is too small to depict on the map but the sample locality is indicated. Southwesterly migration of the magmatic focus from ~11 Ma to present is shown schematically by the heavy black arrow extending from the Indian Creek pluton through the Hannegan caldera to Mount Baker. Basement rocks of the NW Cascades thrust system are shown in light purple, the Cascade Core in light orange, and the Methow–Pasayten Belt in light green. [Colour online.]

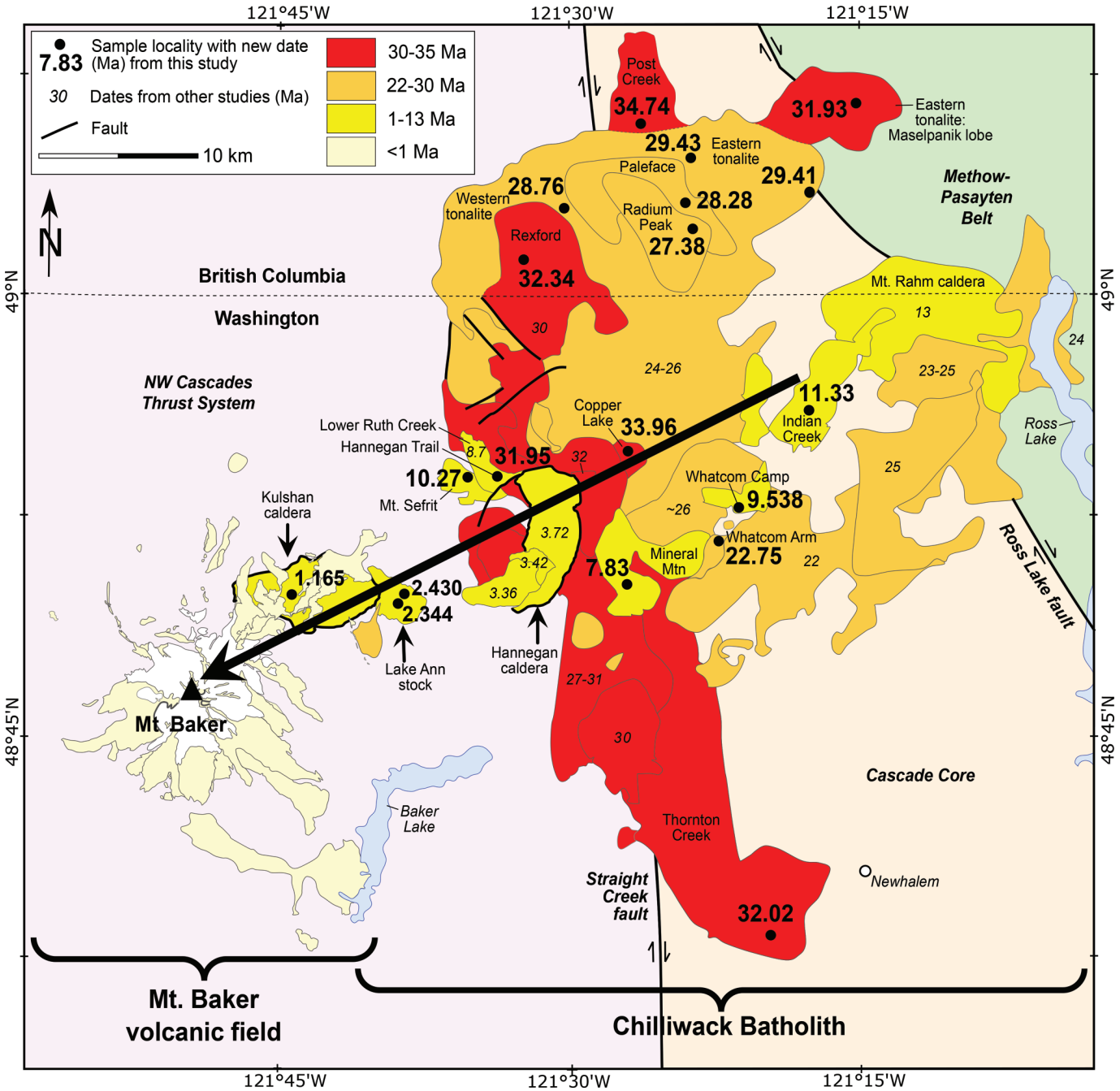

the Juan de Fuca plate has become progressively smaller, younger, and hotter at the trench, resulting in increased buoyancy and resistance to subduction (Riddihough 1984). Consequently, the orthogonal convergence rate between the Juan de Fuca and North American plates has decreased by a factor of five since the initiation of subduction (Verplanck and Duncan 1987). At ~4 Ma, the youngest and most northerly portion of the Juan de Fuca plate detached to create the Nootka fault zone and establish the independent Explorer microplate (Fig. 1), which has ceased to subduct and is in the process of breaking up and becoming captured by North America (Riddihough 1984; Audet et al. 2008; Rohr and Tryon 2010; Rohr 2015).

A bend in the arc axis in Washington subdivides the arc into two major sectors, the Garibaldi Belt (originally defined as extending from Glacier Peak to Bridge River Cones) and the High Cascades (Mount Rainier to Lassen Peak) (Fig. 1). On the basis of geochemical

data, Mullen et al. (2017) recommended including Glacier Peak in the High Cascades suite rather than the Garibaldi Belt. Following du Bray and John (2011), we use the term "ancestral" to refer to magmatism that preceded the "modern" Cascades of approximately 4 Ma to recent. In the High Cascades, ancestral magmatism is preserved in a belt of mainly volcanic rocks known as the Western Cascades located trenchward of the modern arc (Fig. 1). The opposite relationship is observed in the Garibaldi Belt, where ancestral magmas are mainly intrusive and located to the east of the modern arc in a swath known as the Pemberton Belt (Souther 1977; Woodsworth et al. 1991) (Fig. 1). The Garibaldi and Pemberton Belts merge at Mount Meager (Souther and Yorath 1991). The dearth of preserved volcanic rocks in the Pemberton Belt is attributed, in part, to the rapid uplift and erosion that have characterized northern Washington and British Columbia since the late Miocene (Reiners et al. 2002). An along-strike change in the crustal stress regime, from extensional in the High Cascades to compressional in the Garibaldi Belt, is also likely to be a factor in reduced eruptive volumes in the Northern Cascades (Hildreth 2007).

The Northern Cascade Arc was not included in du Bray and John's (2011) assessment of arc evolution due to an apparently uncertain affiliation of these magmas with subduction. However, geochemical data clearly demonstrate that mafic through silicic magmas in the Northern Cascades segment are calc–alkaline with a trace element "arc signature" at least as far north as Mount Meager, British Columbia (e.g., Tabor and Crowder 1969; Berman and Armstrong 1980; Coish and Journeay 1992; Tepper 1991, 1996; Tepper et al. 1993; Mullen and McCallum 2014; Mullen and Weis 2013, 2015; Mullen et al. 2017; authors' unpublished data). On the northern periphery of Mount Meager, recently erupted alkalic mafic lavas at Salal Glacier and Bridge River are related to asthenosphere upwelling through a slab gap along the subducted trace of the Nootka fault (Mullen and Weis 2013). Farther north, two isolated volcanic fields, Franklin Glacier and Silverthrone, lie inboard of the Explorer plate and their relationship to the arc remains uncertain (Mullen et al. 2017).

The most extensive area of plutonic rocks in the Northern Cascades is the Chilliwack batholith, which straddles the Washington–British Columbia border (Figs. 1, 2). The batholith includes at least 55 plutons ranging in area from <1 to >100 km^2 that were emplaced at depths of <10 km, plus subordinate erosional volcanic remnants (Tepper 1991, 1996; Tepper et al. 1993; Tabor et al. 2003). Petrologic and geochemical studies have established that Chilliwack magmas are I-type, medium-K to (less commonly) low-K, and range in composition from gabbro to alaskite with granodiorite and tonalite as the predominant lithologies (Richards and McTaggart 1976; Tepper 1991, 1996; Tepper et al. 1993; Tabor et al. 2003). Radiometric dates previously measured for the Washington sector of the Chilliwack batholith were compiled by Engels et al. (1976) and more recently by Tabor et al. (2003); most were obtained by K–Ar, zircon fission track, multi-grain U–Pb zircon, or Rb–Sr isochron methods. K–Ar dates have been reported for the British Columbia portion of the batholith by Baadsgaard et al. (1961), Richards and McTaggart (1976), and Mathews et al. (1981). Overall, these previously measured dates range from ~2 to 35 Ma.

At the western margin of the Chilliwack batholith, plutonic rocks of the Lake Ann stock are truncated by the eastern margin of the Kulshan caldera (Fig. 2), which represents the easternmost expression of the ~220 km^2 Mount Baker volcanic field (Hildreth 2007). Hildreth et al. (2003) carried out a comprehensive ^{40}Ar/^{39}Ar dating study showing that the Mount Baker volcanic field has been active since ~1.3 Ma, culminating in the ~40 ka to recent andesitic Mount Baker stratocone. Additional ^{40}Ar/^{39}Ar, K–Ar, and isotope dilution – thermal ionization mass spectrometry (ID–TIMS) U–Pb zircon ages (Hildreth et al. 2003; Tucker et al. 2007) extend the magmatic record intermittently back to the 3.722 Ma Hannegan caldera, which is embedded within older Chilliwack plutons and intruded by younger ones (Fig. 2). Advancement of the magmatic focus from the Hannegan caldera to the modern Mount Baker entailed ~25 km of progressive southwesterly migration of the magmatic focus (Hildreth et al. 2003). On the basis of previously determined dates for the Chilliwack batholith, Tepper and Hildreth (2004) suggested that this migration pattern may have initiated as early as ~12 Ma. Magmatic products of the Mount Baker volcanic field are basaltic through rhyodacitic and display a complete compositional overlap with the Chilliwack batholith, demonstrating that the two suites are products of a single causal magmatic phenomenon (Hildreth et al. 2003). As such, the oldest Mount Baker rocks and the youngest Chilliwack rocks could be considered members of both suites.

Basement rocks

The western margin of North America has long been the site of active subduction. The most recent Mesozoic and Cenozoic events have led to the docking of numerous allochthonous terranes, predominantly late Paleozoic to Tertiary in age, that constitute most of the ~35–40 km thick crust upon which the Cascade Arc has been built (Monger et al. 1982; Dickinson 2004; Levander and Miller 2012). In the Northern Cascades, this accreted crust was also intruded by plutons formed in Mesozoic to early Tertiary subduction zones preceding the formation of the Cascade Arc (Monger and Price 2000; Dickinson 2004; Brown and Gehrels 2007).

The Chilliwack–Mount Baker area is underlain by three distinct crustal blocks that are juxtaposed by major Tertiary faults. From west to east, these domains are known as the Northwest Cascades System (NWCS), Cascades Core, and Methow–Pasayten belt (Fig. 2), which are separated by the Straight Creek and Ross Lake faults, respectively. The Mount Baker volcanic field lies entirely within the NWCS, which consists of lithologically diverse and variably metamorphosed Paleozoic to early Cretaceous terranes that are assembled into four major thrust sheets (Tabor et al. 2003; Brown 2012).

The Chilliwack batholith was emplaced mainly into the NWCS and Cascades Core (Fig. 2), although the easternmost Chilliwack intrusions extend into the Methow–Pasayten belt. The Cascades Core is a highly metamorphosed assemblage of Paleozoic to Tertiary accreted terranes that are intruded by mid-Cretaceous to Eocene plutons (e.g., Miller et al. 2009). The terranes of the Methow–Pasayten belt record little to no metamorphism and intrusive rocks are sparse. The Chilliwack batholith is centered upon the north-trending strike-slip Straight Creek fault, and in map view the batholith displays a north–south elongation parallel to the fault (Fig. 2), implying that pluton emplacement was partially controlled by this structure (Woodsworth et al. 1991). However, none of the plutons shows evidence for displacement on the fault (Tepper 1991).

Samples

Age determinations were carried out on 19 samples from the Chilliwack–Mount Baker magmatic focus and 13 samples from neighboring arc plutons to the north and south of this area. Some of the same units were dated by previous studies and the most recently published ages are listed in Table 1. Except for the Kulshan caldera rhyodacite tephra, all of the samples are biotite- and (or) hornblende-bearing, fine- to medium-grained granitoids; additional petrographic details are provided in Table 1.

North of the Chilliwack batholith, new dates were obtained on the Fall Creek stock at Mount Meager, the Hicks Lake pluton, the Mount Barr batholith, and the Silver Creek stock. These new dates complement existing dates for the Rogers Creek intrusive complex and the Harrison Lake, Doctors Point, and Salal Creek plutons (Fig. 1*b*). The Fall Creek sample is a rounded lithic clast ejected from the conduit wall during the 2360 before present subplinian eruption of Mount Meager (Campbell et al. 2013). The Mount Barr batholith has been subdivided into four phases (Richards and McTaggart 1976) and the dated sample represents the largest (Conway) phase. South of the Chilliwack batholith, new ages were

Table 1. Samples and dating results.

[a]Rock unit	Sample no.	Latitude (°N)	Longitude (°W)	Rock type	[b]Previous dates (Ma)	Previous dating method	[c]Reference	Date (Ma) from this study
Chilliwack-Mt. Baker magmatic focus								
Kulshan caldera	08-MB-124	47°12.90′	122°13.13′	rhyodacite tephra	1.149±0.010	$^{40}Ar/^{39}Ar$ plag	4	**1.165±0.013**
Lake Ann: central	06-MB-70	48°49.794′	121°39.261′	bio–hbl grdi	2.75±0.13	$^{40}Ar/^{39}Ar$ bio	4	**2.344±0.021**
Lake Ann: upper	06-MB-68	48°49.823′	121°38.700′	bio–hbl grdi	—	—	—	**2.430±0.016**
Mineral Mountain	RWT269–87	48°50.2′	121°27.2′	bio granite	~7.3 to 8.1	multi-grain U–Pb zircon	3	**7.83±0.06**
Whatcom Camp	CB87–50	48°52.2′	121°22.3′	hbl–bio granite	—	—	—	**9.538±0.065**
Mt. Sefrit	CB82–103	48°53.7′	121°35.1′	hbl qz diorite	22.86±0.05	Rb–Sr isochron	1	**10.27±0.06**
Indian Creek	CB87–37	48°56.4′	121°18.2′	hbl qz mzdi	12.1±0.8	K–Ar bio	5	**11.33±0.08**
Whatcom Arm	CB87–33	48°51.7′	121°22.3′	hbl grdi	—	—	—	**22.75±0.17**
Radium Peak stock	15-PB-01	49°02.436′	121°24.133′	bio–hbl grdi	27±2	K–Ar bio	2	**27.38±0.12**
Paleface stock	15-PB-02	49°02.919′	121°24.273′	bio–hbl grdi	—	—	—	**28.28±0.15**
Western tonalite	15-PB-10	49°04.944′	121°31.736′	tonalite	—	—	—	**28.76±0.14**
Eastern tonalite	CB89–1	49°03.2′	121°17.2′	bio–hbl grdi	30, 29±2	K–Ar bio	2	**29.43±0.16**
	15-PB-06	49°05.062′	121°25.666′	bio–hbl tonalite	—	—	—	**29.41±0.13**
Eastern tonalite: Maselpanik lobe	15-PB-15	49°07.201′	121°15.017′	hbl–bio tonalite	—	—	—	**31.93±0.16**
Hannegan Trail	CB82–151	48°53.8′	121°33.6′	porph hbl–bio tonalite	8.7	zircon FT	1	**31.95±0.24**
Thornton Creek	TH-20	48°37.98′	121°19.50′	qz diorite	~29–35	K–Ar, multi-grain U–Pb and FT zircon	3	**32.02±0.16**
Rexford stock	15-PB-11	49°03.089′	121°34.423′	bio–hbl diorite	27±2	K–Ar bio	2	**32.34±0.17**
Copper Lake	CB87–112	48°54.8′	121°27.3′	hbl qz diorite	34.03±0.91	Rb–Sr isochron	1	**33.96±0.18**
Post Creek stock	CB87–10	49°05.7′	121°26.3′	hbl–bio qz monzonite	27±2	K–Ar bio	2	**34.74±0.24**
Copper Ridge Lookout	CB87–116	48°54.5′	121°27.8′	hbl–bio tonalite	—	—	—	**86.91±0.43**
North of Chilliwack batholith								
Fall Creek stock	FCS	50°40.91′	123°30.67′	qz monzonite	10.1±1.2	K–Ar bio	7	**6.646±0.046**
Mount Barr batholith: Conway phase	15-PB-13	49°15.462′	121°40.760′	hbl–bio qz monzonite	18.5±1.8	K–Ar bio	8	**18.13±0.10**
Silver Creek stock	15-PB-14	49°14.920′	121°36.175′	bio–hbl qz diorite	36±4	K–Ar hbl	2	**23.77±0.10**
Hicks Lake pluton	15-PB-12	49°21.722′	121°42.683′	hbl granite	25±1.4	K–Ar bio	2	**26.23±0.16**
South of Chilliwack batholith								
Cascade Pass dike	15-PB-16	48°28.642′	121°04.198′	porph hbl–bio qz diorite	18.5±3, 18.8±2	K–Ar hbl, K–Ar bio	6	**32.78±0.28**
Index batholith	ISM-IX	47°48.281′	121°31.249′	hbl–bio grdi	~33–36	K–Ar, Rb–Sr, multi-grain U–Pb and	6	**33.26±0.19**
	CC11–26	47°47.878′	121°30.875′	tonalite		FT zircon		**33.53±0.15**
Squire Creek stock	15-PB-19b	48°7.866′	121°36.308′	sulfide-bearing bio–hbl tonalite	~33–36	K–Ar, multi-grain U–Pb and FT zircon	6	**35.84±0.16**
Grotto batholith	16-EM-01	47°43.031′	121°23.365′	tonalite	25.7±3 Ma	K–Ar hbl	9	**24.14±0.45**
Snoqualmie batholith, northern sector	16-EM-03	47°39.677′	121°22.889′	bio tonalite	23.0±1.2 Ma	K–Ar hbl	9	**23.87±0.15**

[a]Chilliwack batholith nomenclature follows the usage of Tepper et al. (1993) and Tepper (1996, 1991) in Washington and Richards and McTaggart (1976) in British Columbia.

[b]Most recent best age estimate or measured age (or range), with 2σ errors listed on individual measurements (where reported in the original reference). Where necessary, K–Ar dates have been corrected to 1976 IUGS constants following Dalrymple (1979).

[c]1. Tepper (1991), 2. Richards and McTaggart (1976), 3. Tabor et al. (2003), 4. Hildreth et al. (2003), 5. Mathews et al. (1981), 6. Tabor et al. (2002), 7. Stevens et al. (1982), 8. Baadsgaard et al. (1961), 9. Tabor et al. (1993)

Abbreviations: plag, plagioclase; bio, biotite; hbl, hornblende; grdi, granodiorite; qz, quartz; mzdi, monzodiorite; porph, porphyritic; FT, fission track.

Fig. 3. Tera–Wasserburg $^{207}Pb/^{206}Pb$ vs. $^{238}U/^{206}Pb$ diagrams for samples from the Chilliwack–Mount Baker magmatic focus. Each ellipse represents the 2σ error associated with a single zircon spot analysis. Data are not corrected for common Pb. Lower intercept ages and Concordia ages (also listed in Table 1) were calculated using the filled gray ellipses (N is the number of analyses). MSWD is the mean square of weighted deviates; for Concordia ages, it includes both equivalence and concordance (indicated by subscript C + E). Data points lying outside the main cluster of data are shown as open dashed ellipses and were excluded from age calculations. Filled red data points are inherited grains. Red points in (*a*) are from two inherited grains; those in (*b*) are from a single inherited grain. [Colour online.]

determined on the Cascade Pass dike, the Index, Grotto, and the northern Snoqualmie batholiths, and the Squire Creek stock (Tabor et al. 1993, 2002, 2003) (Fig. 1*b*). Sample localities are shown in Figs. 1*b* and 2. Due to disturbance by advances of the Cordilleran ice sheet, the plinian fallout from the Kulshan caldera-forming eruption is preserved only far south of the caldera (Hildreth et al. 2004). The sample studied here was collected ~200 km south of Mount Baker at Sumner, Washington, where the fallout is known as the Lake Tapps tephra (Westgate et al. 1987) (Fig. 1*b*).

Analytical methods

U–Th–Pb analyses by LA–ICP–MS

Zircons were separated at the Laboratoire Magmas et Volcans (LMV) using standard techniques of crushing, sieving, and isodynamic magnetic separation, followed by Wilfley table or heavy liquids (bromoform and methylene iodide). Approximately 50 zircons per sample were mounted in epoxy disks and ground and polished to expose crystal interiors. Cathodoluminescence (CL) imaging was conducted at LMV on selected samples using a JEOL JSM-5910LV scanning electron microscope (SEM) (JEOL Ltd., Tokyo, Japan). U–Th–Pb isotope data were measured by LA–ICP–MS at LMV. Zircons were ablated using a Resolution M-50 (Resonetics LLC, Nashua, New Hampshire, USA) equipped with a 193 nm ultrashort-pulse Atlex excimer laser system (ATL Lasertechnik GmbH, Wermelskirchen, Germany) (Müller et al. 2009) coupled to a Thermo Element XR SF-ICP-MS (Thermo Scientific, Bremen, Germany). Helium carrier gas was supplemented with N_2 prior to mixing with Ar for sensitivity enhancement (Paquette et al. 2014). The laser was operated with a spot diameter ranging from 33 to 60 μm, a repetition rate of 3 Hz, and a fluence of 2.5 to 5.5 J/cm^2. Other instrumental operating conditions and data acquisition parameters are detailed in Table S1[1].

The Element ICP–MS was tuned to maximize the ^{238}U intensity and minimize ThO^+/Th^+ (<1.5%) using the SRM 612 glass (National Institute of Standards and Technology, Gaithersburg, Maryland, USA). The signals of ^{204}Pb (+Hg), ^{206}Pb, ^{207}Pb, ^{208}Pb, ^{232}Th, and ^{238}U were acquired during each analysis. After pre-ablating each spot, background levels were measured on-peak with the laser off for ~30 s, followed by ~60 s of measurement with the laser firing, and then ~30 s of washout time. Reduction of raw data was carried out using the GLITTER software package of Macquarie Research Ltd (Sydney, Australia) (van Achterbergh et al. 2001). Isotope ratios (with ^{235}U calculated as $^{238}U/137.88$) were corrected for laser-induced and instrumental mass fractionation via sample-standard bracketing using the GJ-1 zircon ($^{206}Pb/^{238}U$ age of 601 Ma; Jackson et al. 2004) that was analyzed four times at the beginning and end of each analytical session and twice after each set of 8 samples. Concentrations of U, Th, and Pb were calculated by normalization to the certified composition of GJ-1 (Jackson et al. 2004). $^{206}Pb/^{238}U$ ratios were corrected for ^{230}Th disequilibrium following Schärer (1984) by using the Th/U ratio of the whole rock (where data are available) as that of the magma or by assuming a value of 3.5 ± 0.5 that represents the range defined by Chilliwack granitoids (Tepper 1991, 1996; Tepper et al. 1993; Mullen 2011; authors' unpublished data). Data are not corrected for common Pb. Tera–Wasserburg $^{207}Pb/^{206}Pb$ vs. $^{238}U/^{206}Pb$ diagrams were generated for each sample using the Isoplot/Ex v. 2.49 software of Ludwig (2001) (BGC, Berkeley, California, USA) (Figs. 3–5). Error ellipses for each point are shown at the 2σ level and incorporate both internal and external uncertainties. Data points were pooled to calculate a date and associated 2σ error for each sample (reported in Fig. 3 and Table 1) using Isoplot. The Harward 91500 zircon (1065 Ma; Wiedenbeck et al. 1995) was analyzed along with the samples, twice at the beginning and end of each session, to independently monitor the external precision and accuracy of the measurements. The Concordia age for 132 analyses of 91500 conducted over the course of the study was 1063.9 ± 2.4 Ma (2σ including decay constant errors; MSWD = 2.1 including concordance + equivalence) as shown in Table S2[1].

Results

Zircon morphology, petrography, and CL imaging

The analyzed zircons are pale pink to pale yellow or colorless, and most grains are transparent and euhedral with habits ranging from prismatic to acicular. Zircon was detected in thin sections of several samples but is most abundant in the Lake Ann samples. CL images (Fig. 6) display fine oscillatory, patchy, and complex zoning patterns that are consistent with magmatic growth (Corfu et al. 2003) and lack obvious signs of xenocrystic cores or overgrowths.

U–Th–Pb data

The complete dataset of measured U–Th–Pb isotope ratios and abundances is provided in Table S2[1]. Concordia ages are reported for six samples (Table 1, Figs. 3–5). For the other samples, the data define linear correlations on $^{207}Pb/^{206}Pb$ versus $^{238}U/^{206}Pb$ diagrams (Figs. 3–5) that extend between a lower Concordia intercept age (reported in Table 1) and a common Pb composition at the upper intercept (Tera and Wasserburg 1972). We interpret the Concordia and lower intercept ages as those of magma crystallization. Multiple spots were analyzed on some individual zircon grains, and the resulting ages were within error. Overall, Th/U ratios for most of the zircons are from 0.16 to 2.0, with several outliers as low as 0.04. U and Th contents are typically ~30–1300 ppm and ~10–1900 ppm, respectively, although a few analyses extend up to ~2800 ppm U and ~3400 ppm Th. These values are typical of igneous rocks (Lopez-Sanchez et al. 2016). Except for the Cascade Pass dike sample, where zircons define a bimodal age distribution, inherited zircons older than magma crystallization ages are rare and occur as only one or two grains in a few samples.

Chilliwack–Mount Baker magmatic focus

The new dates are presented in order of increasing age. The rhyodacite tephra of Lake Tapps yielded a lower intercept age of 1.165 ± 0.013 Ma (Table 1, Fig. 3*a*), in excellent agreement with Hildreth et al.'s (2003) date of 1.149 ± 0.010 Ma ($^{40}Ar/^{39}Ar$ plagioclase) from a Kulshan caldera rhyodacite ignimbrite, and confirming the work of Westgate et al. (1987) indicating that the Kulshan caldera was the most probable source of the Lake Tapps tephra. Three older inherited zircons were also present in the sample (red points in Figs. 3*a*, 3*b*); two grains at ~3 Ma (three spots analyzed) and one grain at ~200 Ma (three spots analyzed). Th/U ratios for the main zircon population are 0.3–1.2, and the inherited zircons are indistinguishable with Th/U = 0.3–0.4 for the older grain and

[1]Supplementary data are available with the article through the journal Web site at http://nrcresearchpress.com/doi/suppl/10.1139/cjes-2017-0167.

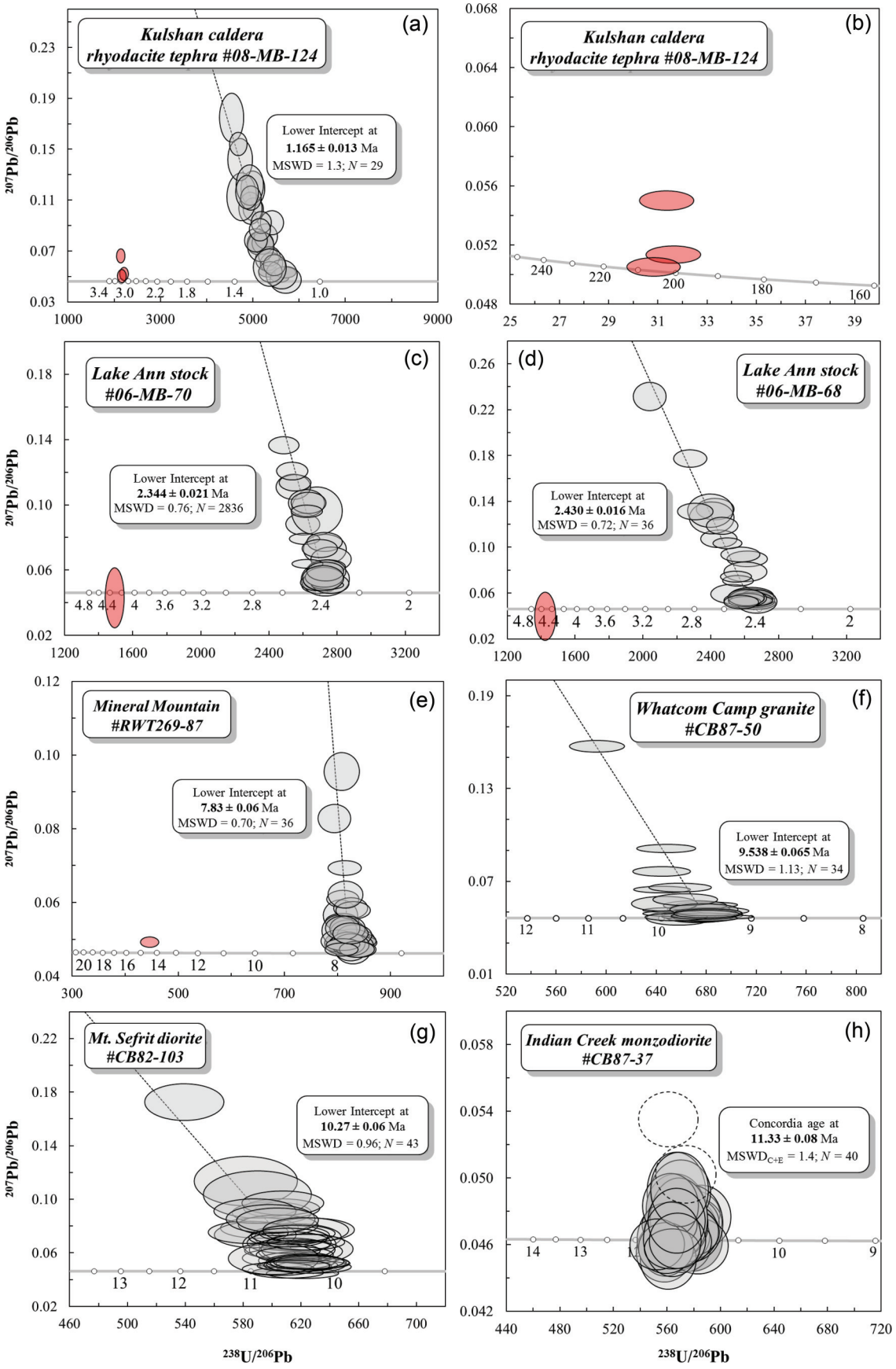

Fig. 3 (*continued*).

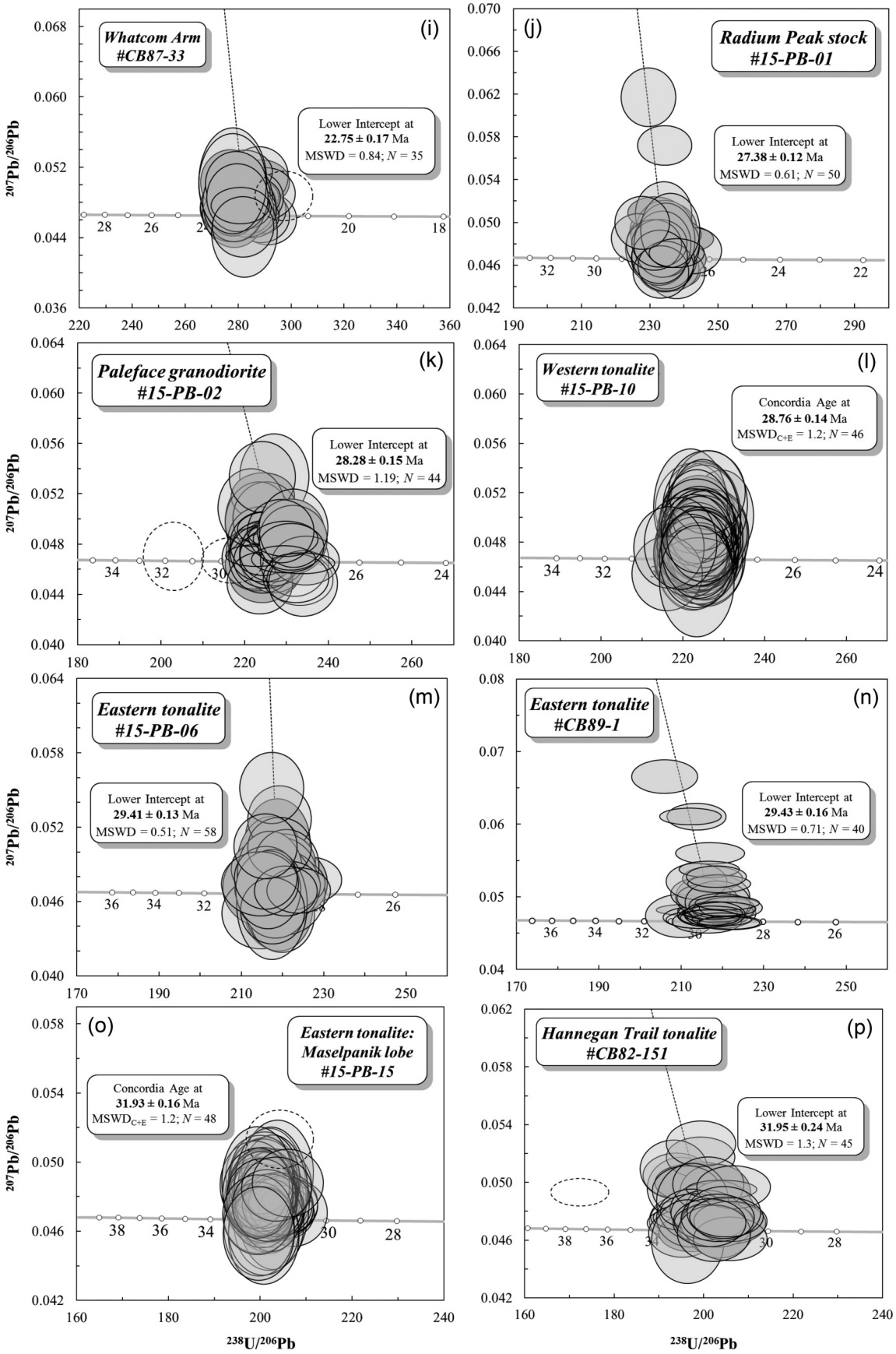

Fig. 3 (*concluded*).

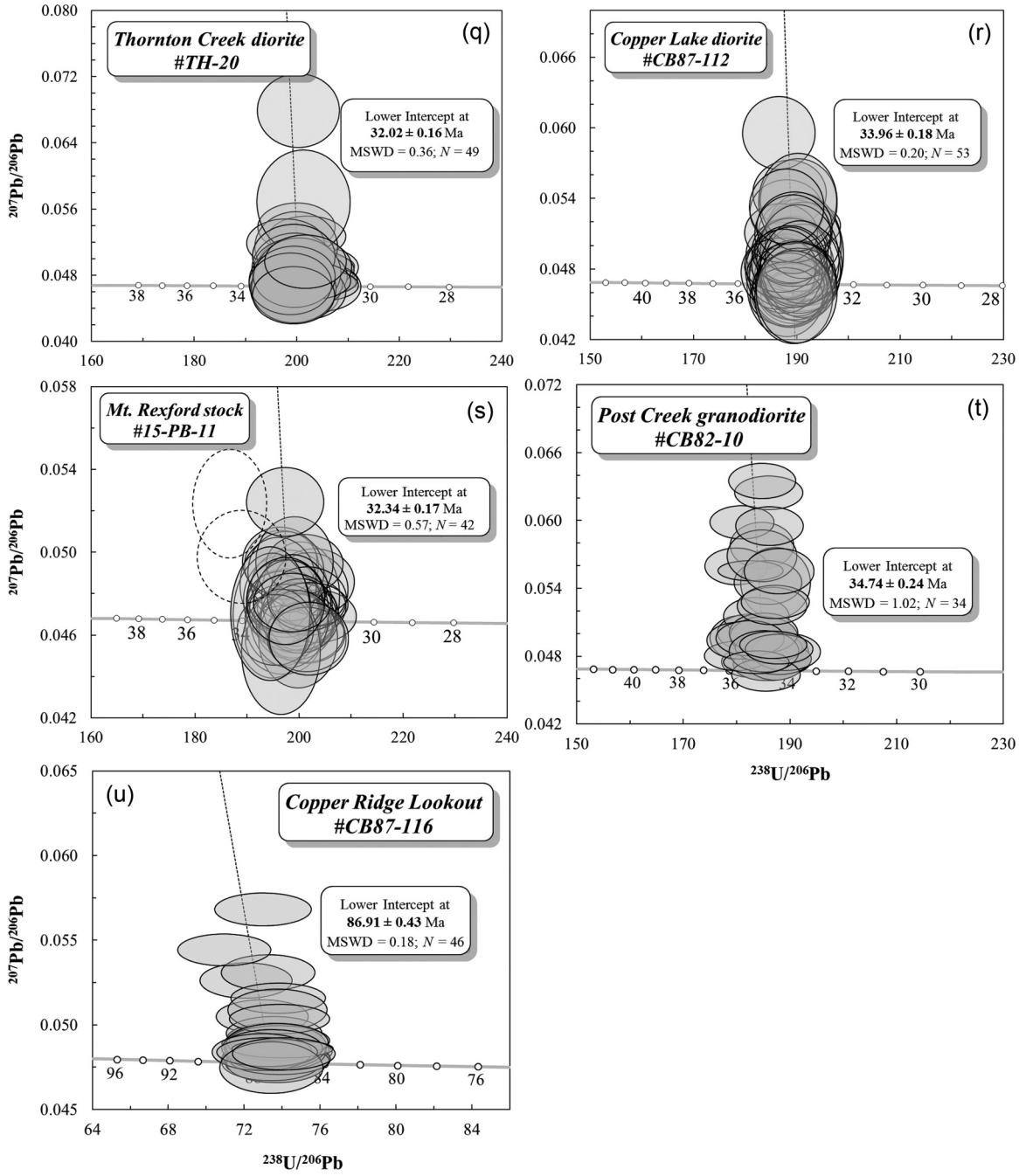

0.6–0.7 for the younger grains. Dates for two granodiorites from different parts of the Lake Ann stock, which was cut by the Kulshan caldera eruption, are outside of respective 2σ errors at 2.344 ± 0.021 and 2.430 ± 0.016 Ma (Table 1, Figs. 3*c*, 3*d*). Both new ages are younger than the 2.75 ± 0.13 Ma $^{40}Ar/^{39}Ar$ biotite age of Hildreth et al. (2003). The sample collected from the upper part of the intrusion (06-MB–68) crystallized between 49 and 123 ka before the sample from the center (06-MB–70), evidence for incremental growth of this magma body. Each Lake Ann sample also yielded a single inherited zircon grain at ~4.3 and 4.5 Ma (red points in Figs. 3*c*, 3*d*). The inherited grains display Th/U ratios of ~0.5, overlapping with those of the main zircon populations (~0.4 to 0.9).

A zircon separate from a granite of the Mineral Mountain pluton (#RWT269–87) gave a lower intercept age of 7.83 ± 0.06 (Table 1, Fig. 3*e*) that is consistent with dates of ~7.3 to 8.1 Ma (multi-grain U–Pb TIMS) and 6.5 ± 2.6 Ma (fission track) previously measured on the same separate (Tabor et al. 2003 and references therein). However, we also identified a single inherited grain of ~14–15 Ma (red point in Fig. 3*e*) with a Th/U ratio of 0.5 that overlaps with the main zircon population (~0.4 to 1.6). Farther to the northeast, the previously undated Whatcom Camp granite (Tepper 1991) returned a lower intercept age of 9.538 ± 0.065 Ma (Table 1, Fig. 3*f*). A quartz diorite from the Mount Sefrit pluton gave a lower intercept age of 10.27 ± 0.06 Ma (Table 1, Fig. 3*g*), in agreement with our recalculated Rb–Sr isochron age of 10.08 ± 0.29 Ma for the biotite–plagioclase–clinopyroxene–whole rock data of Tepper (1991) for an associated gabbro. In the eastern sector of the batholith, the Indian Creek pluton returned a 11.33 ± 0.08 Ma lower intercept age (Table 1, Fig. 3*h*) for a quartz monzo-

Fig. 4. Tera–Wasserburg $^{207}Pb/^{206}Pb$ vs. $^{238}U/^{206}Pb$ diagrams for intrusions north of the Chilliwack batholith. Each ellipse represents the 2σ error associated with a single zircon spot analysis. Data are not corrected for common Pb. Lower intercept ages and Concordia ages (also listed in Table 1) were calculated using the filled gray ellipses (N is the number of analyses). MSWD is the mean square of weighted deviates; for Concordia ages, it includes both equivalence and concordance (indicated by subscript C + E). Data points lying outside the main cluster of data are shown as open dashed ellipses and were excluded from age calculations. Filled red data points are inherited grains. [Colour online.]

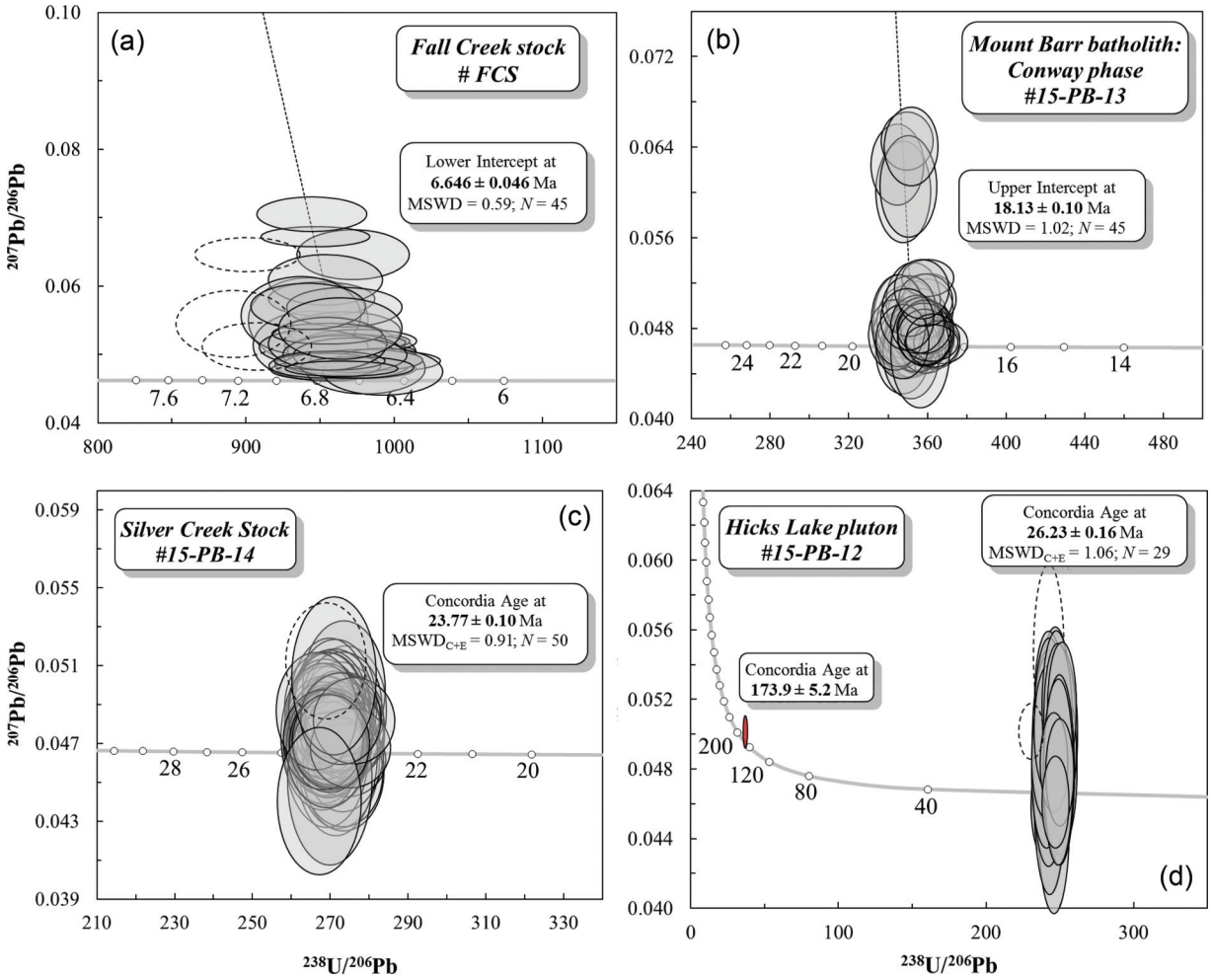

nite, within the respective 2σ errors of previous dates of 12.1 ± 0.8 (K–Ar biotite, Mathews et al. 1981) and 10.8 ± 1.8 (K–Ar hornblende, Engels et al. 1976). The previously undated granodiorite of Whatcom Arm (Tepper 1991) gave a lower intercept age of 22.75 ± 0.17 Ma (Table 1, Fig. 3*i*).

In British Columbia, a lower intercept age of 27.38 ± 0.12 Ma for a granodiorite from the Radium Peak stock (Table 1, Fig. 3*j*) is consistent with the 27 ± 2 Ma K–Ar biotite age reported by Richards and McTaggart (1976). Samples from the previously undated Paleface stock and Western tonalite (Richards and McTaggart 1976) were collected ~10 km apart, yet returned ages of 28.28 ± 0.15 Ma (lower intercept) and 28.76 ± 0.14 Ma (Concordia), respectively (Table 1, Figs. 3*k*, 3*l*), nearly within error. For the Eastern tonalite, two of the three dated samples, collected ~10 km apart, are within error at 29.41 ± 0.13 and 29.43 ± 0.16 Ma (Table 1, Figs. 3*m*, 3*n*) and both fall within the 2σ uncertainties of K–Ar biotite determinations (30 ± 2 and 29 ± 2 Ma; Richards and McTaggart 1976). However, the third Eastern tonalite sample (#15-PB–15), which was collected farther northeast (Fig. 2), is at least 2.23 million years older with a Concordia age of 31.93 ± 0.16 Ma (Table 1, Fig. 3*o*). In recognition of this difference, we refer to the older portion of the Eastern tonalite as a separate "Maselpanik lobe" (Fig. 2). Th/U ratios for all three Eastern tonalite samples are 0.2–0.8, except for a few analyses from one sample (#CB89–1) that are as low as 0.04. The low Th/U reflects elevated U contents (up to ~1270 ppm) relative to other analyses from the same sample (~60 to 580 ppm U). Nevertheless, the low-Th/U points are not associated with any age discrepancy outside of analytical error.

A zircon fission track age of 8.7 Ma was previously reported for the Hannegan Trail porphyritic tonalite (Tepper 1991), but our sample from this unit gave a significantly older age (lower intercept) of 31.95 ± 0.24 Ma (Table 1, Fig. 3*p*). The largest and southernmost pluton in the Chilliwack batholith, Thornton Creek, was previously dated by a variety of methods and most results were in the ~29 to 35 Ma range (Tabor et al. 2003 and references therein). Our new lower intercept age of 32.02 ± 0.16 Ma for a quartz diorite (Table 1, Fig. 3*q*) lies within the same range. Th/U ratios from this sample are 0.3 to 0.7, with the exception of a single low value of 0.04 due to high U (~480 ppm) compared with other grains (maximum ~320 ppm). For the Copper Lake pluton, a 33.96 ± 0.18 Ma lower intercept age for a hornblende quartz diorite (Table 1, Fig. 3*r*) is within error of Tepper's (1991) Rb–Sr isochron date of 34.03 ± 0.91 Ma (biotite–hornblende–plagioclase–whole rock) for a diorite sample.

Identical K–Ar biotite ages of 27 ± 2 Ma have been reported for the Post Creek and Mount Rexford stocks of British Columbia (Richards and McTaggart, 1976). However, both of our new ages (lower intercept) are significantly older, 32.34 ± 0.17 Ma for Mount

Fig. 5. Tera–Wasserburg $^{207}Pb/^{206}Pb$ vs. $^{238}U/^{206}Pb$ diagrams for intrusions south of the Chilliwack batholith. Each ellipse represents the 2σ error associated with a single zircon spot analysis. Data are not corrected for common Pb. Lower intercept ages and Concordia ages (also listed in Table 1) were calculated using the filled gray ellipses (N is the number of analyses). MSWD is the mean square of weighted deviates; for Concordia ages, it includes both equivalence and concordance (indicated by subscript C + E). Data points lying outside the main cluster of data are shown as open dashed ellipses and were excluded from age calculations. Filled red data points are inherited grains. [Colour online.]

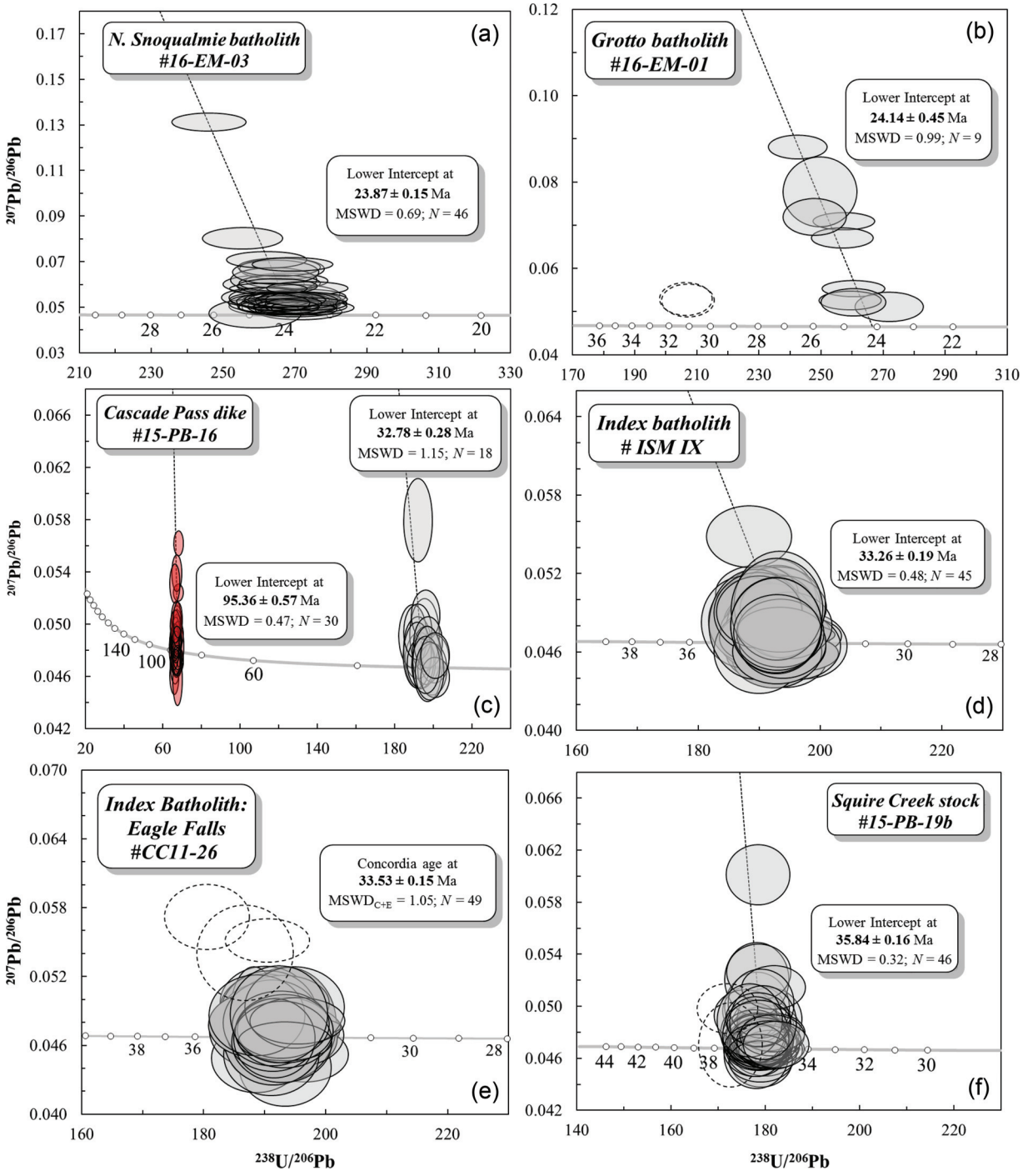

Rexford and 34.74 ± 0.24 for Post Creek (Table 1, Figs. 3*s*, 3*t*). Our date for the Post Creek stock is the oldest measured on Chilliwack batholith samples.

A new date of 86.91 ± 0.43 Ma for Tepper's (1991) tonalite of Copper Ridge Lookout (Table 1, Fig. 3*u*) indicates that this unit is not part of the Chilliwack batholith, but this date does fall within the ~71–96 Ma range reported for Cascade Core plutonic basement rocks, which are also predominantly tonalitic (Miller et al. 2009). Th/U ratios of 0.2 to 0.6 are also consistent with an igneous origin.

The new dating results were used to color-code the individual phases of the Chilliwack batholith by age (Fig. 2). For plutons not dated in this study, we used ages compiled and recommended by Tabor et al. (2003) (Table S3[1]). Diagrams displaying the new dates on east–west and north–south profiles (Fig. 7) highlight spatial shifts in magmatism through time.

Fig. 6. Cathodoluminescence images of representative dated zircon grains from (*a*, *b*) the Lake Ann stock (sample #06-MB–70) and (*c*–*f*) the Fall Creek stock (sample #FCS). Circles indicate analyzed spots and corresponding numbers refer to analytical points in Table S2[1].

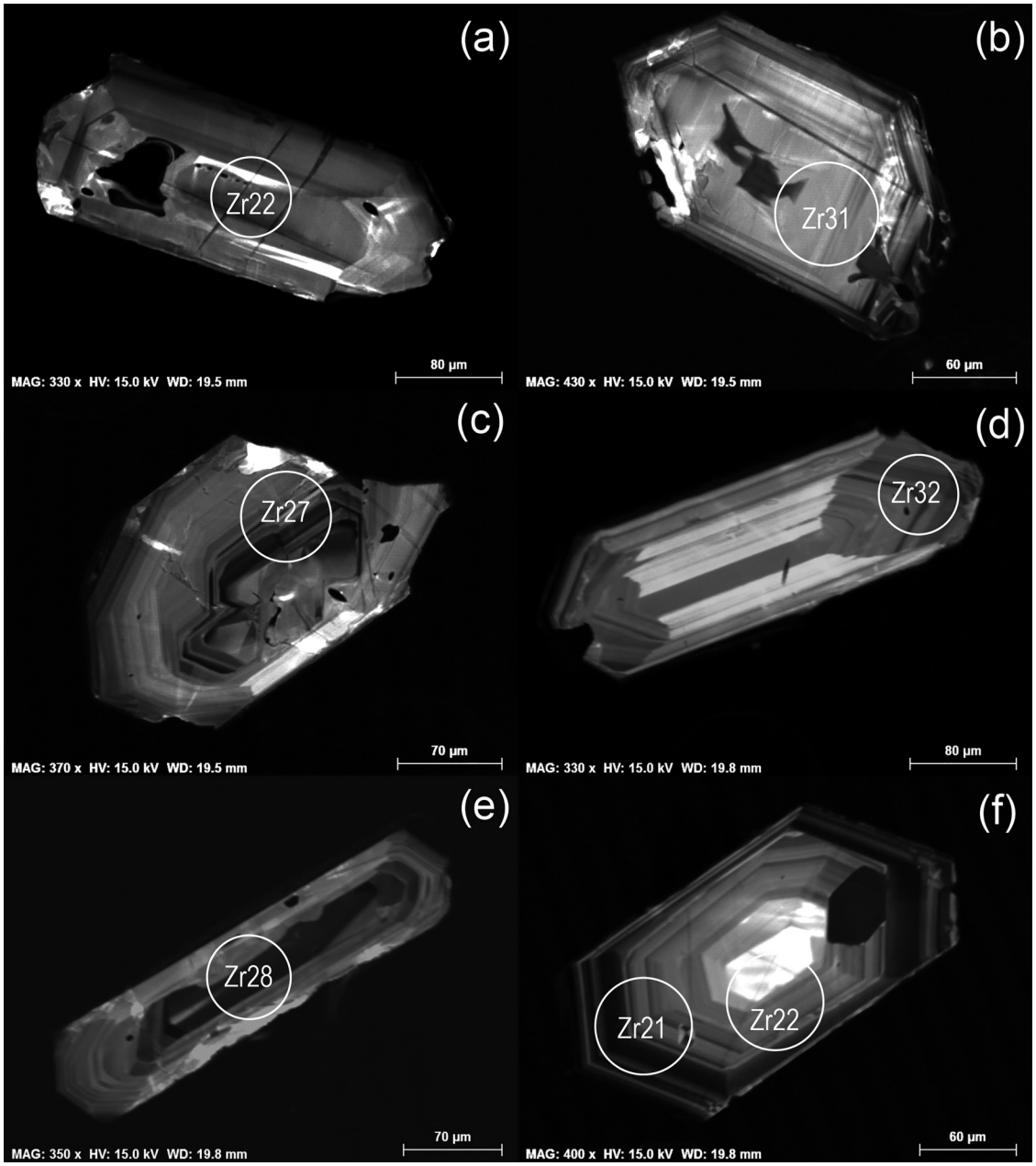

The exposed areas of individual plutons were calculated digitally from geologic maps and are plotted as a function of time (Fig. 8) as a first-order proxy for the "apparent intrusive flux" (de Silva et al. 2015). Since the third dimensions of the plutons are unknown, the calculated fluxes should be viewed as estimates. Except for caldera fills and the area covered by the Mount Baker volcanic field (shown for reference), the few small volcanic remnants in the Chilliwack are omitted from Fig. 8 because of uncertainties in intrusive to extrusive ratios (e.g., Paterson and Ducea 2015) and unknown pre-erosive dimensions.

North of the Chilliwack batholith

The northernmost sample dated for this study, a quartz monzonite from the Fall Creek stock underlying Mount Meager, gave a lower intercept age of 6.646 ± 0.046 Ma (Table 1, Fig. 4*a*) that is significantly younger than the previous 10.1 ± 1.2 (K–Ar biotite) determination of Stevens et al. (1982). A new 18.13 ± 0.10 Ma lower intercept age (Table 1, Fig. 4*b*) for a quartz monzonite from the Conway phase of the Mount Barr batholith, the largest of four mapped phases, overlaps with Baadsgaard et al. (1961)'s K–Ar biotite date of 18.5 ± 1.8 Ma. Our result is also in the range of K–Ar biotite dates reported for two of the three other phases of the batholith, Wahleach Lake and Mount Barr (~16–22 Ma) (Richards and McTaggart 1976). The Silver Creek stock, located just north of the Chilliwack batholith, was once thought to be the oldest in the Pemberton Belt based on a K–Ar hornblende date of 36 ± 4 Ma (Richards and McTaggart 1976). However, the new date for Silver Creek, measured on a quartz diorite, is considerably younger at 23.77 ± 0.10 Ma (Table 1, Fig. 4*c*). A granite from the Hicks Lake pluton yielded a Concordia age of 26.23 ± 0.16 Ma (Table 1, Fig. 4*d*), comparable to the 25 ± 1.4 Ma K–Ar biotite date of Richards and McTaggart (1976). One inherited zircon grain of ~174 Ma was also identified (red ellipse, Fig. 4*d*). The Th/U ratio of the inherited

Fig. 7. Dates for the Chilliwack–Mount Baker magmatic focus versus (*a*) longitude and (*b*) latitude. Dates from this study are shown as red filled circles, except for inherited zircons shown as red asterisks. 2σ error bars are smaller than symbols. Previous age determinations are shown as gray filled circles with corresponding 2σ error bars (Tabor et al. 2003 and references therein; Hildreth et al. 2003; Tucker et al. 2007). [Colour online.]

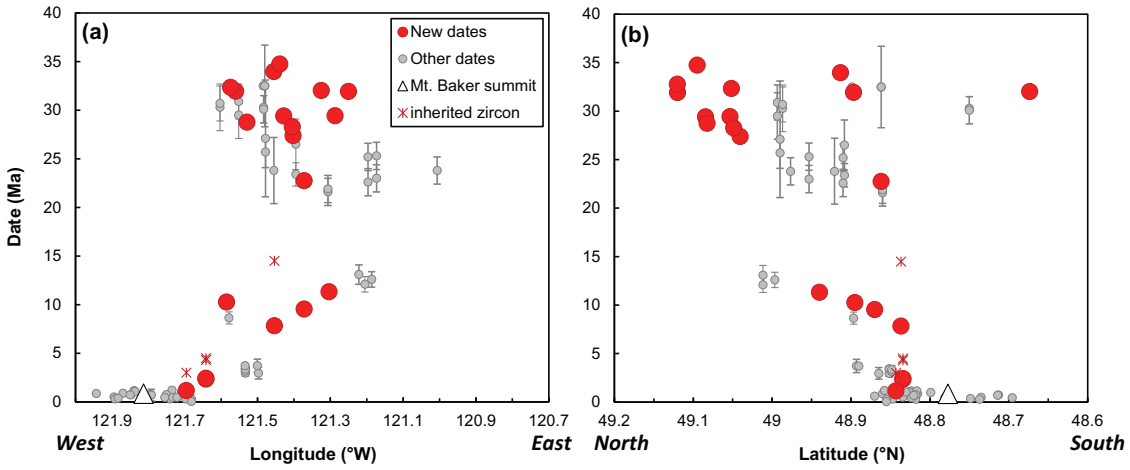

Fig. 8. (*a*) Stacked histogram of the areas (km²) defined by Northern Cascades intrusive rocks, binned into 1 million year intervals. Pluton areas are tabulated in Table S3[1]. Gray line is the convergence rate of the Farallon plate system (cm/year) from Verplanck and Duncan (1987) with scale on the right-side *y* axis. (*b*–*d*) The same data for pluton areas shown in (*a*) but subdivided into three regions: (*b*) Chilliwack–Mount Baker magmatic focus, (*c*) South of Chilliwack, and (*d*) North of Chilliwack. The area covered by <1 Ma volcanic rocks of Mount Baker is shown for reference in yellow in (*b*). Note the different *y*-axis scales associated with each panel. Although few intrusive rocks south of the Chilliwack batholith date between ~25 and 32 Ma (panel *c*), a number of volcanic and volcaniclastic rock units lie in this range, most notably the Ohanapecosh Formation, as indicated by the horizontal black arrow (Jutzeler et al. 2014; Tabor et al. 2000; Schasse 1987; Evarts et al. 1987). [Colour online.]

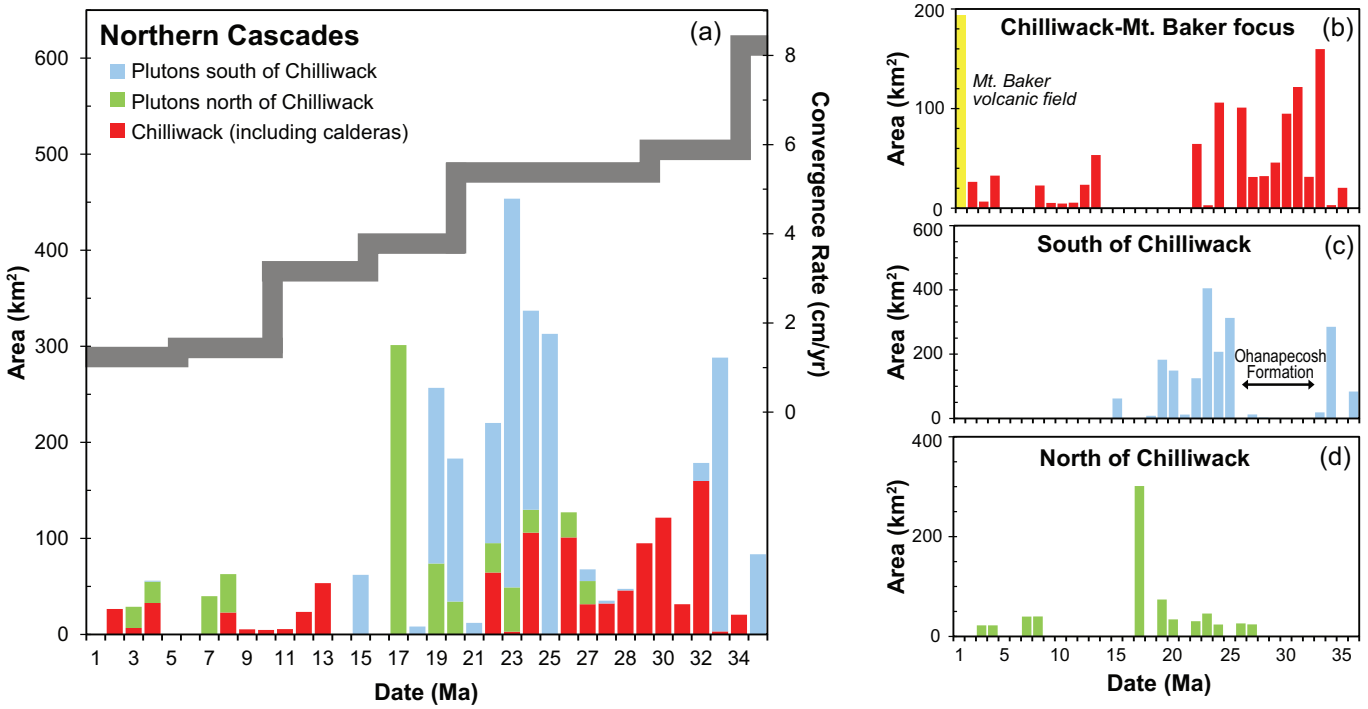

grain (~0.4) overlaps with the 0.2 to 0.5 range defined by the main zircon population.

South of the Chilliwack batholith

Multiple K–Ar and zircon fission track dates obtained for the Snoqualmie batholith indicate that it generally decreases in age from ~25 Ma in the north to ~18 Ma in the south (Tabor et al. 1993 and references therein). Our new lower intercept age of 23.87 ± 0.15 Ma for a tonalite from the northern Snoqualmie batholith (Fig. 5*a*) agrees with a K–Ar hornblende date of 23.0 ± 1.2 Ma for a nearby sample locality (Tabor et al. 1993; sample #5). The Grotto batholith is located on the northern boundary of the Snoqualmie batholith, and it has long been hypothesized that the two intrusions represent a single body based upon similar ranges of previously measured ages (Tabor et al. 1993, and references therein). An intensive search for zircon in our tonalite from the Grotto batho-

lith produced only nine grains, the fewest in our study. Nevertheless, these grains yielded a lower intercept age of 24.14 ± 0.45 Ma (Fig. 5*b*), identical (within error) to our new age for the northern Snoqualmie batholith and confirming that the two intrusions are most likely continuous at depth.

The quartz diorite sample from the Cascade Pass dike is unique in this study in that the zircon data delineate two distinct age populations, both of which display well-defined lower intercepts. About 40% of the data define an age of 32.78 ± 0.28 Ma and the other ~60% define an age of 95.36 ± 0.57 Ma (Fig. 5*c*). The younger zircon grains are stubby, prismatic, yellow to pink, and tend to be smaller than the older zircons, which are pink and more elongate. Th/U ratios of the younger population (0.4–0.6) overlap with those of the older population (0.3–0.5), both of which are typical of igneous rocks. We report the younger age (32.78 Ma) as that of magma crystallization and the older age (95.36 Ma) as that of an inherited component. The new solidification age for the dike is significantly older than the previously accepted age of ~18 Ma for the Cascade Pass dike (Tabor et al. 2002).

New dates for two samples from different parts of the Index batholith, a granodiorite and tonalite, are within analytical error at 33.26 ± 0.19 and 33.53 ± 0.15 Ma (Table 1, Figs. 5*d*, 5*e*) and are consistent with the ~34 Ma best age estimate for the batholith based on multiple K–Ar, multi-grain U–Pb zircon, Rb–Sr, and zircon fission track determinations that lie in the ~33–36 Ma range (Tabor et al. 1993 and references therein). Th/U ratios are 0.2–0.9, except for one analysis with a ratio of 0.04 that reflects a slightly elevated U content (~740 ppm). Our oldest date for Northern Cascade arc magmas was measured on a tonalite from the Squire Creek stock, which gave a lower intercept age of 35.84 ± 0.16 Ma (Fig. 5*f*) that overlaps with a number of K–Ar, multi-grain U–Pb zircon, and zircon fission track dates of ~33 to 36 Ma (Tabor et al. 2002 and references therein).

All of the new dates from this study are plotted versus latitude in Fig. 9, along with previous radiometric dates for Northern Cascades volcanic and plutonic rocks from Mount St. Helens to Silverthrone. The areas defined by Northern Cascades intrusive rocks, calculated digitally from geologic maps (Richards and McTaggart 1976; Woodsworth 1977; Ray and Coombes 1985; Evarts et al. 1987; Schasse 1987; Monger 1989; Journeay and Friedman 1993; Tabor et al. 1993, 2000, 2002; du Bray et al. 2011), are plotted versus age in Fig. 8 to approximate the intrusive flux for this segment of the arc. Areas are tabulated in Table S3[1].

Discussion

Discrepancy between new and previous dates

About half of the new dates differ well outside of 2σ errors from previous age determinations on the same unit. For a given analytical method, however, the previous dates are systematically neither older nor younger. Argon loss and (or) the lower closure temperature of the K–Ar system could explain why several of the new U–Pb zircon dates are older than previous K–Ar dates (e.g., Cascade Pass dike, Rexford, Post Creek, and Eastern tonalite), but these processes cannot account for why both new dates for the Lake Ann stock are younger than the $^{40}Ar/^{39}Ar$ biotite date of Hildreth et al. (2003). In contrast to those samples, a number of the new U–Pb zircon dates agree well with previous K–Ar ages (e.g., Index, Snoqualmie, Squire Creek, Radium Peak, Hicks Lake, Mount Barr, and Indian Creek). The significant difference between the new U–Pb date (31.95 Ma) and the zircon fission track date (8.7 Ma, Tepper 1991) for the Hannegan Trail unit may be the result of resetting by the adjacent Lower Ruth Creek unit, which was also dated at 8.7 Ma by Rb–Sr isochron (Tepper 1991).

Provenance of inherited zircons

The inherited zircons from the Lake Ann and Mineral Mountain intrusions (Figs. 3*c*–3*e*), as well as the younger (~3 Ma) inherited zircon population from the Kulshan caldera (Fig. 3*a*), are several millions of years older than magma crystallization ages, yet within the overall range defined by the Chilliwack batholith. The Th/U ratios of the inherited grains are consistent with a magmatic growth (Lopez-Sanchez et al. 2016) and are indistinguishable from the Th/U ratios of other zircons in the same samples. We consequently interpret these inherited zircons as xenocrysts derived from earlier arc magmatic pulses.

Fig. 9. New dates from this study (red circles) vs. latitude; 2σ error bars are smaller than symbols. Vertical dashed line at 4 Ma distinguishes the modern from the ancestral Cascades. Other radiometric age determinations for Cascade Arc volcanic rocks (yellow diamonds) and plutonic rocks (pink circles) are shown with 2σ error bars where reported and are from Berman and Armstrong (1980), du Bray et al. (2011), Green et al. (1988), Hildreth et al. (2003), Hildreth and Lanphere (1994), Jicha et al. (2009), Jutzeler et al. (2014), Mathews et al. (1981), Mattinson (1977), Ray (1986), Reiners et al. (2000), Richards and McTaggart (1976), Tucker et al. (2007), Wanless et al. (1978), Evarts et al. (1987), Tabor et al. (2003, 2002, 2000, 1993), Schasse (1987), Phillips (1987), and du Bray and John (2011). K–Ar dates are corrected to 1976 International Union of Geological Sciences constants (following Dalrymple 1979) as necessary. [Colour online.]

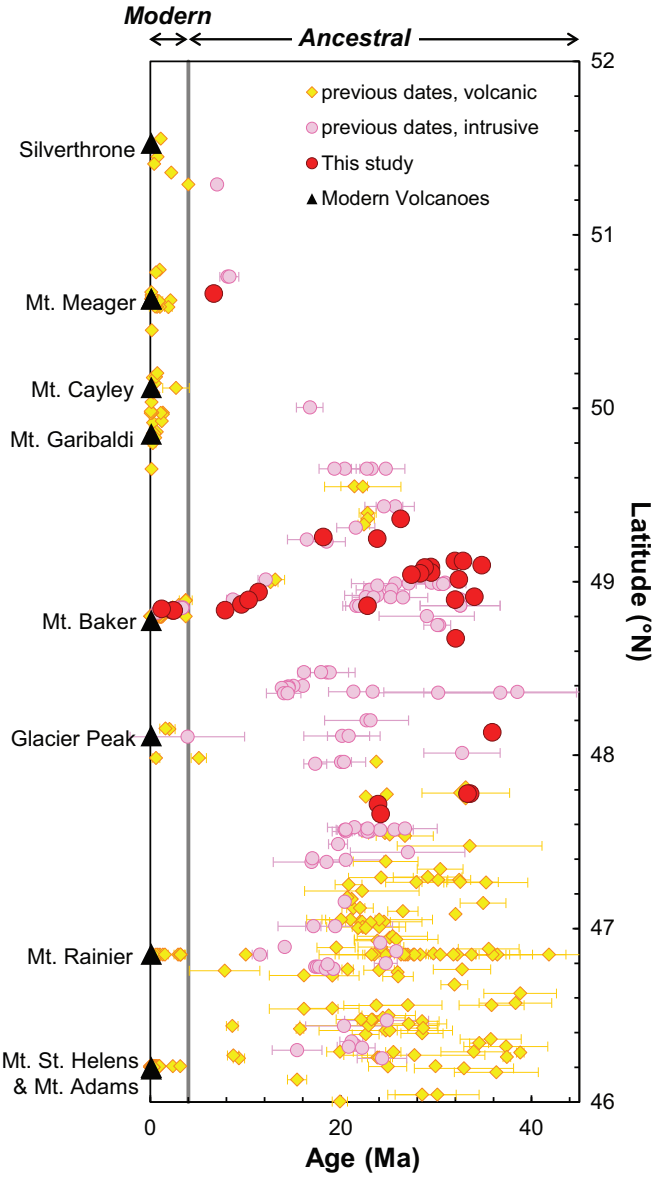

With a significantly older age of ~200 Ma, the second inherited zircon in the Kulshan caldera sample (Fig. 3*b*) is consistent with a xenocryst derived from basement rock. However, the age of this xenocryst does not match the age ranges of the three units truncated by the caldera eruption (Tabor et al. 2003), i.e., the Middle Jurassic to Early Cretaceous Nooksack Formation (~180–100 Ma, Brown and Gehrels 2007), the Paleozoic Chilliwack Group (~370–410 Ma, Brown et al. 2010), and the Lake Ann stock (~2.3–2.4 Ma, this study). Furthermore, none of the other NWCS units displays a ~200 Ma detrital zircon peak (Brown and Gehrels 2007). However, the Nooksack Formation is correlative with the Harrison terrane in British Columbia (Monger and Journeay 1994; Tabor et al. 2003), which extends back to middle Triassic (Mahoney et al. 1995) and does encompass the age of the xenocryst. Alternatively, structural reconstructions and seismic reflection–refraction data indicate that the NWCS occupies only the upper ~10 km of the crust and is underlain by a middle to lower crust composed of the Wrangellia terrane onto which the NWCS was obducted (Zelt et al. 1993; Monger and Journeay 1994; Monger and Price 2000; Miller et al. 1997; Brown 2012). Wrangellia is presently exposed to the west on Vancouver Island, and its presence beneath the Chilliwack–Mount Baker area is further supported by the emplacement of Mount Baker within a structural window in which the NWCS thrust sheets were removed to reveal underlying rocks of the Nooksack Formation and Wells Creek volcanics that formed in close association with Wrangellia (Monger and Journeay 1994; Tabor et al. 2003). Major constituents of Wrangellia are the 203 to 164 Ma igneous rocks of the Bonanza Arc (Nixon and Orr 2007), overlapping with the age of the inherited zircon in the Kulshan caldera sample. Th/U ratios of the inherited zircon are also consistent with a magmatic origin.

The Hicks Lake pluton is underlain by rocks of the Middle Triassic to Lower Cretaceous Harrison terrane and its metamorphosed equivalent, the Slollicum schist (Monger 1989; Mahoney et al. 1995). The single Jurassic (~174 Ma) inherited zircon identified in our Hicks Lake sample (Fig. 4*d*) overlaps with the age range of these basement rocks. A Th/U ratio of 0.4 for the inherited grain is typical of igneous rocks and consistent with the predominantly volcanic and volcaniclastic origin of the Harrison terrane (Mahoney et al. 1995).

The Cascade Pass dike sample contains by far the largest proportion (~60%) of xenocrystic zircons, which define a lower intercept age of 95.36 ± 0.57 Ma (Fig. 5*c*). Of several units in the Cascade Core crustal block that were intruded by the dike, only the Eldorado orthogneiss, which has a reported age of ~88–92 Ma based on zircon multi-grain fraction U–Pb TIMS dating (Tabor et al. 2003 and references therein), is a close match to the age of the xenocrysts. Th/U ratios for the Cretaceous zircon population are typical of magmatic rocks, consistent with derivation from an orthogneiss. The other intruded units are the 60–70 Ma Skagit Gneiss Complex and the Triassic Cascade River schist and Marblemount pluton (Tabor et al. 2003).

Temporal evolution of Chilliwack–Mount Baker magmatism

The twenty new dates for the Chilliwack batholith delineate an episodic magmatic history that was punctuated by an early flare-up and later interrupted by a prolonged lull. We subdivide magmatism into three main phases. Phase 1 (~35 to 30 Ma) defines the highest intrusive flux in the lifetime of the Chilliwack–Mount Baker magmatic focus (Fig. 8). The earliest magmatism is recorded by the Post Creek stock, the northernmost pluton in the batholith, at 34.74 Ma (Fig. 2). Within less than 3 million years, activity spread to the center (Copper Lake, 34.03 Ma) and the southernmost reaches of the batholith to form largest intrusive body, Thornton Creek (118 km^2, Tabor et al. 2003), at 32.02 Ma (Fig. 2, 7*b*). Phase 1 magmatism was predominantly concentrated in a north-trending belt in the western sector of the batholith, roughly coinciding with the Straight Creek fault (Figs. 2, 7*a*). Farther east, the Maselpanik lobe of the Eastern tonalite is centered on the Ross Lake fault zone (Fig. 2).

Over the following ~8 million years (Phase 2, ~30–22 Ma), the magmatically active zone gradually broadened to the east (Fig. 7*b*). The intrusive flux (Fig. 8) remained steady but was slightly lower than during the flare-up of Phase 1. Whatcom Arm (22.75 Ma) was the final intrusion emplaced before a lull lasting ~11 million years.

The end of the lull, and the beginning of Phase 3, was marked by the emplacement of the Indian Creek pluton (11.33 Ma) in the eastern sector of the batholith (Fig. 2). Indian Creek also initiated a pattern of southwesterly migration of the magmatic focus that persisted over a distance of ~45 km to culminate at the modern Mount Baker stratocone (Fig. 7*a*). Compared with prelull Chilliwack activity, postlull magmatism was more sporadic (Fig. 8) and the intrusive flux was ~5 times lower (14 vs. 63 km^2/million years; calculations in Table S3[1]). Following emplacement of the Indian Creek pluton, the magmatic focus shifted to Whatcom Camp (9.538 Ma), followed by Mineral Mountain (7.83 Ma) and then the Hannegan caldera at 3.72 Ma (Fig. 2). During the ~7.6 million years that elapsed between Indian Creek and the Hannegan caldera, the migration distance was ~20 km, corresponding to an average migration rate of ~2.6 mm/year. The Mount Sefrit pluton also falls within Phase 3 at 10.27 Ma, but it is an exception to the migration pattern as it is located farther west than predicted for its age (Fig. 2, 7*a*). However, as one of the rare mafic plutons in the Chilliwack batholith (Tepper 1996), the peripheral location of Mount Sefrit is consistent with the observation that mafic magmas in the Cascades tend to occur on the fringes of the main magmatic focus (Hildreth 2007). From ~3.7 Ma to the present, migration persisted an additional ~25 km from Hannegan caldera to the modern Mount Baker (Hildreth et al. 2003), following an azimuth similar to that defined by the first ~7.6 million years of migration, but at an accelerated rate of ~6.7 mm/year.

The ~3.7 million years of migration in the Hannegan–Mount Baker sequence was attributed by Wells and McCaffrey (2013) to clockwise rotation of the arc crust, augmented by slab rollback. Global Positioning System vectors indicate that the arc is rotating clockwise with respect to stable North America about a pole in eastern Oregon, and paleomagnetic data confirm that this rotation has been occurring at a similar rate for at least the past ~15 million years (McCaffrey et al. 2007, 2013; Wells and McCaffrey 2013). This crustal rotation is driven by a combination of Basin and Range extension and dextral shear due to the oblique subduction of the Farallon plate (Wells and Heller 1988). Rotation around the eastern Oregon pole would have displaced the ancestral Southern and Central Cascades (the Western Cascades) to the west of modern High Cascades and the Pemberton Belt to the east of the modern Garibaldi Belt, both of which are observed (Fig. 1).

In the Chilliwack–Mount Baker area, the modern vector for arc rotation, ~3.5 mm/year along a northeasterly azimuth (Wells and McCaffrey 2013), is comparable with both the rate (2.6 mm/year) and direction of the first ~8 million years of migration, from Indian Creek to the Hannegan caldera. The accelerated migration of the past 3.7 million years requires an added velocity component that Wells and McCaffrey (2013) ascribed to slab rollback, as is occurring in the modern arc (Schellart et al. 2010). The onset of slab rollback may be related to the separation of the buoyant Explorer plate from the Juan de Fuca plate at ~4 Ma (Riddihough 1984), which would have had the effect of removing a kinematic constraint on the Juan de Fuca plate, causing an increase in the dip of the slab and enhancing rollback.

The temporal decrease in magma productivity in the Chilliwack batholith, as indicated by the general reduction in intrusive flux through time (Fig. 8), correlates with the ~5-fold decrease in the normal component of the convergence rate from 35 Ma to the present (Verplanck and Duncan 1987). Trace element data for Chilliwack–Mount Baker magmas support this explanation, as magmas emplaced after the lull have a more muted "subduction

Fig. 10. Map of northern Washington (WA) and southern British Columbia (B.C.) showing intrusive bodies (pink) and modern volcanic centers (red triangles) with a superimposed slab migration model. Dashed red contours (labeled 35, 25, 15, and 5 Ma) are based on the maximum ages of intrusive bodies in each sector (see Figs. 3–5 for age details) and record the temporal location of the northern edge of the subducted slab relative to the North American plate (NAM). Major intrusions and volcanic complexes are numbered: 1. Tatoosh, 2. Snoqualmie, 3. Index, 4. Grotto, 5. Squire Creek, 6. Cloudy Pass, 7. Cascade Pass, 8. Chilliwack, 9. Mt. Barr, 10. Silver Creek, 11. Harrison Lake, 12. Hicks Lake, 13. Podunk Creek, 14. Coquihalla complex, 15. Doctors Point, 16. Rogers Creek, 17. Fall Creek, 18. Salal Creek. Spreading centers, transform faults, and trenches are based on Botros and Johnson (1988), Rohr (2015), and McCrory et al. (2014). In this model (after Rohr 2015), the Explorer–North American–Pacific triple junction is a zone of distributed shear between the strike-slip Queen Charlotte fault (QCF) and Dellwood–Revere fault (DRF). Seismic tomography places the present-day northern edge of the Explorer plate at the Brooks Peninsula Fault Zone (BPFZ), which extends inland from the southern boundary of the Winona basin (WB) (Audet et al. 2008) and beneath the Alert Bay volcanic field (AB). Modern volcanic centers: ST, Silverthrone; FG, Franklin Glacier; BR, Bridge River; SG, Salal Glacier; MM, Mount Meager; MC, Mount Cayley; MG, Mount Garibaldi; MB, Mount Baker; GP, Glacier Peak; MR, Mount Rainier. Other abbreviations: V, Vancouver; S, Seattle; NFZ, Nootka Fault Zone; SFZ, Sovanco Fracture Zone; JDF, Juan de Fuca plate; PAC, Pacific plate; EXP, Explorer plate. [Colour online.]

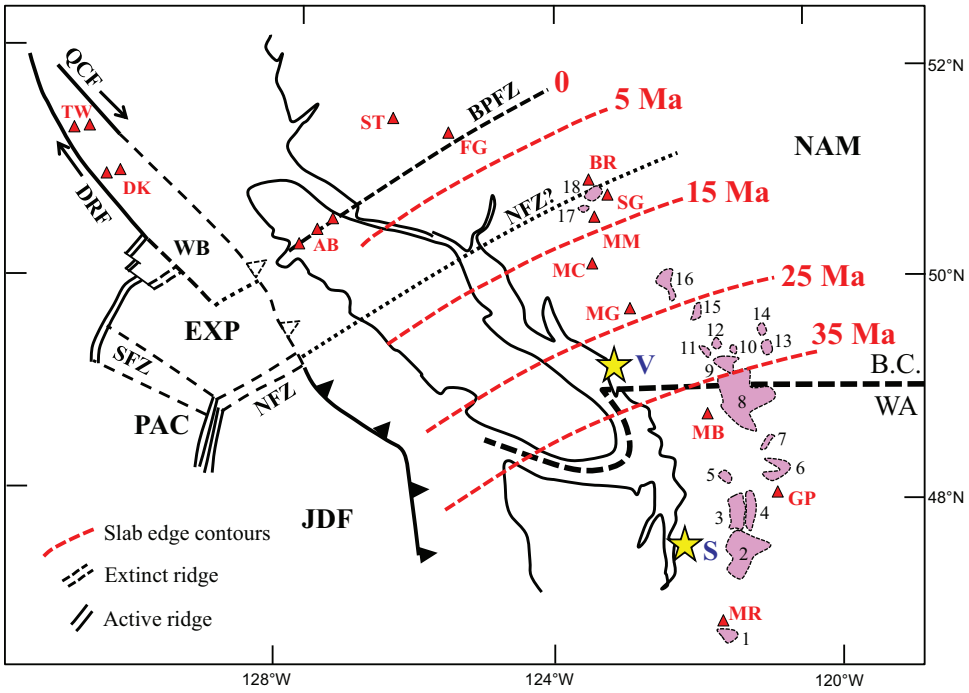

signature" such as lower Ba/Nb, lower B/Be, and higher incompatible element concentrations (e.g., Nb, Th) (Tepper 2002). These differences point to a declining fluid flux from the slab and decreased mantle melt fractions as subduction slowed and the slab became younger and warmer. Because the Farallon plate was larger, older, and cooler earlier in the history of the arc (Schellart et al. 2010), the slab would have dipped at a steeper angle, which could account for the more westerly location of the earliest-formed Chilliwack plutons (Fig. 2, Fig. 7*a*). The decrease in convergence rate does not appear to be related to the ~11 million year lull in Chilliwack magmatism because, as discussed in the next section, this lull appears to be restricted to the Chilliwack–Mount Baker magmatic focus.

Regional Patterns

South of the Chilliwack–Mount Baker magmatic focus, few intrusive rocks have yielded dates within the ~25–32 Ma age range (Fig. 8*c*), in apparent contrast to the Chilliwack batholith. However, a number of volcanic and volcaniclastic rock units date within this interval, most notably the areally extensive (>400 km^2) Ohanapecosh Formation near Mount Rainier (Schasse 1987; Tabor et al. 2000; Jutzeler et al. 2014) (Fig. 9). Farther to the south, magma output rates calculated from volcanic rock exposures in the Central and Southern Cascade Arc display a temporal decrease that has also been attributed to the convergence rate decrease (Verplanck and Duncan 1987; Duncan and Kulm 1989; Priest 1990; Sherrod and Smith 2000; du Bray and John 2011). However, peak output rates occurred at ~25 to 17 Ma (du Bray and John 2011), slightly younger than in the Chilliwack batholith (Fig. 8).

The magmatic lull in the Chilliwack–Mount Baker area from ~22 to 11 Ma does not appear to be an arc-scale phenomenon, as plutons were emplaced both to the immediate north and the south of the Chilliwack batholith during this interval (Fig. 9). Our new date of 18.13 ± 0.1 Ma for the Conway phase of Mount Barr batholith, which lies adjacent to the northern margin of the Chilliwack batholith, falls within the ~16–22 Ma range determined by Richards and McTaggart (1976) on the basis of low-precision K–Ar dating. Farther to the north, the Doctors Point pluton was emplaced as recently as 19.3 ± 1.6 Ma (Ray 1986) and the Rogers Creek intrusive complex has been dated at 16.7 ± 2.7 Ma (Fig. 9, 10; Wanless et al. 1978). Immediately south of the Chilliwack batholith, K–Ar hornblende ages for the Mount Buckindy pluton range from 14.0 ± 1.8 to 16 ± 0.4 Ma (Tabor et al. 2002 and references therein), and four phases of the Tatoosh intrusive suite in the Mount Rainier area were recently dated at 17.5–19.2 Ma by SIMS U–Pb zircon (du Bray et al. 2011). However, with very few volcanic or plutonic rocks falling in the 15–5 Ma age range (Fig. 9), the area to the south of the Chilliwack batholith appears to have entered a period of quiescence at about the same time as the re-establishment of Chilliwack magmatism (by ~11 Ma).

Compared with the Northern Cascades, where the oldest magmas are ~35–36 Ma, a number of K–Ar and ^{40}Ar/^{39}Ar ages of up to ~40 Ma have been reported for volcanic rocks in the central Ore-

gon and Mount Rainier – Mount St. Helens regions of the Cascades (Fig. 9; compilations of Sherrod and Smith 2000; du Bray et al. 2006; du Bray and John 2011) that place arc initiation at up to ~6 million years earlier than in the north. However, most of the >35 Ma ages for the Southern and Central Cascades are associated with large uncertainties and many were measured on samples for which existing geochemical evidence is insufficient to establish an arc affinity (e.g., the Goble volcanics; Beck and Burr 1979; Madsen et al. 2006). New dating and geochemical studies will be required to determine exactly when and where arc magmatism first initiated. Nevertheless, within the resolution provided by currently available data for the Southern and Central Cascades, arc magmatism appears to have initiated at around the same time all along the arc, as far north as the Chilliwack batholith (Fig. 9).

To the north of the Chilliwack batholith, maximum pluton ages rapidly diminish northwards, indicating progressively more recent onset of arc magmatism (Fig. 9). We propose that this pattern reflects the northerly migration of the of the Juan de Fuca/Explorer plate system (relative to North America) to its current position (Fig. 10). Although the northern edge of the Explorer plate offshore is conventionally placed at the termination of the Queen Charlotte transform fault (as shown in Fig. 1), recent detailed geophysical surveys (Rohr and Tryon 2010; Rohr 2015) have shown that the Revere–Dellwood fracture represents an offset continuation of the Queen Charlotte transform and that the Winona basin is an isolated fragment of oceanic crust that is not being subducted. In this model, the magmatic centers of the Tuzo Wilson and Dellwood Knolls are not true spreading centers but the result of localized extensional regimes in the zone between the two strands of the transform (Fig. 10). Consequently, we place the northern edge of the offshore plate system at the southern end of the Winona basin in the vicinity of the Brooks Peninsula, a conclusion that is also supported by seismic imaging (Cassidy et al. 1998; Audet et al. 2008). Magnetic anomalies indicate that the northern edge of the plate system has remained stable in its current position for the past ~6.5 Ma (Riddihough 1984). However, the magnetic anomalies needed to reconstruct the position of the triple junction prior to that time have been subducted (e.g., Atwater and Molnar 1973; Wilson 1988; Wright et al. 2016). The only constraints provided by extant anomalies are that the Juan de Fuca–Pacific spreading ridge extended at least as far north as the latitude of central Oregon at ~42 Ma (Wells et al. 2014), the Washington–Oregon boundary at ~38 Ma, and southern Vancouver Island by ~21 Ma (Atwater and Molnar 1973). Several reconstructions of the triple junction have been proposed based on occurrences of magmas possibly related to slab windows (Breitsprecher et al. 2003; Madsen et al. 2006; Wright et al. 2016) and models for the formation and accretion of the Siletz terrane (McCrory and Wilson 2013; Wells et al. 2014). However, these reconstructions differ significantly in their placement of the triple junction through time relative to the coastline. We argue that the best temporal record of the position of the subducting plate relative to the North America plate is given by the ages of Northern Cascade Arc magmas. The northerly younging of arc plutons is consistent with the model in Fig. 10, which shows the Farallon plate present beneath all of the Cascades as far north as the Chilliwack batholith by ~35 Ma. Farther north at Mount Meager, the new 6.46 Ma date for the Fall Creek stock indicates that the subducting plate only arrived beneath the northern Pemberton Belt nearly 30 million years later. The motion of the Juan de Fuca plate relative to the North American plate based upon the slab migration contours shown in Fig. 10 is ~1 cm/year, consistent with the detailed plate model of Madsen et al. (2006).

Conclusions

We present a refined magmatic chronology for silicic plutons of the Northern Cascade Arc from Snoqualmie batholith in central Washington to Fall Creek in southern British Columbia, with emphasis on samples from the Chilliwack batholith – Mount Baker magmatic focus. The new LA–ICP–MS U–Pb zircon dates are associated with significantly smaller uncertainties than previous age determinations, and many differ outside of analytical error from previously published ages. The new dates provide evidence for major variations in magmatic flux over the lifetime of the Chilliwack–Mount Baker magmatic focus and demonstrate that the southwesterly migration pattern first identified in the ~3.7 Ma to present interval between the emplacement of the Hannegan caldera and the modern Mount Baker volcanic field began ~7 million years earlier. New dates for other plutons of the Pemberton Belt constrain the location of the northern edge of the Juan de Fuca – Explorer plate system (relative to North America) over the last 35 million years. Our main conclusions are as follows:

(1) The highest intrusive flux is associated with the magmatic flare-up of Phase 1 (30–35 Ma). Phase 1 intrusions are largely located in the western part of the arc and extend from Post Creek stock, the northernmost pluton in the Chilliwack batholith, to Thornton Creek, the largest and southernmost pluton. Most of the intrusions are concentrated in a north–south trending belt straddling the Straight Creek fault. South of the Chilliwack batholith, Phase 1 units include the Index batholith, Cascade Pass dike, and Squire Creek stock.

(2) Slightly lower-flux magmatism persisted uninterrupted throughout Phase 2 (30–22 Ma), during which the magmatically active zone in the Chilliwack batholith broadened to the east. Phase 2 includes the Snoqualmie and Grotto batholiths to the south and the Silver Creek and Hicks Lake plutons to the north of the Chilliwack batholith.

(3) The ~13 million year period of essentially continuous activity of Phases 1 and 2 was followed by a nearly 11 million year period of dormancy (lull) in the Chilliwack–Mount Baker magmatic focus, during which magmatism was active only to the north and south of the Chilliwack batholith. New dates confirm that the Mount Barr batholith, located immediately north of the Chilliwack, and the Tatoosh magmatic suite south of the Chilliwack, formed during the lull.

(4) Postlull magmatism (Phase 3) resumed in the east-center of the Chilliwack batholith with the Indian Creek pluton at 11 Ma. However, Phase 3 magmatism was intermittent and the intrusive flux was reduced by a factor of five. Phase 3 magmas define a striking pattern of ~45 km of southwesterly migration over ~11 million years, extending the pattern recorded within the 3.7 Ma to present Mount Baker – Lake Ann stock – Hannegan caldera suite. Arc rotation since the Miocene can account for the rate and direction associated with the first ~7 million years of migration. Doubling of the migration rate at ~4 Ma coincided with separation of the Explorer plate and the onset of Juan de Fuca plate rollback.

(5) The oldest dates for Cascade Arc magmatism rapidly decrease to the north of the Chilliwack batholith. This pattern is consistent with reflecting the northerly migration of the northern edge of the Farallon – Juan de Fuca – Explorer plate system relative to the North American plate. From the Chilliwack batholith to the south, the earliest magmatism is consistently in the ~35–40 Ma range, indicating that Farallon plate subduction was well-established along the entire arc by this time.

(6) A general decrease in intrusive flux through time mirrors the pattern defined by volcanic rocks in the Central and Southern Cascades. These observations are consistent with the progressive reduction in the convergence rate of the subducting plate, which has become younger and hotter at the trench, and therefore more resistant to subduction, through time.

Acknowledgements

We wish to thank C. Fonquernie (LMV) for assistance with zircon separations and J.-M. Hénot (LMV) for cathodoluminescence imaging. We appreciate the thorough reviews of Associate Editor C. McFarlane and an anonymous reviewer, and thank A. Polat for editorial handling. We gratefully acknowledge financial support from LabEx ClerVolc and a Région Auvergne fellowship to E.K.M. This is LabEx ClerVolc contribution 277.

References

Atwater, T., and Molnar, P. 1973. Relative motion of the Pacific and North American plates deduced from sea-floor spreading in the Atlantic, Indian and South Pacific Oceans. *In* Proceedings of the Conference on Tectonic Problems of the San Andreas Fault System. *Edited by* R.L. Kovach and A. Nur. Stanford University, Publications in the Geological Sciences, Vol. 13, pp. 136–148.

Audet, P., Bostock, M.G., Mercier, J.P., and Cassidy, J.F. 2008. Morphology of the Explorer–Juan de Fuca slab edge in northern Cascadia: Imaging plate capture at a ridge-trench-transform triple junction. Geology, **36**(11): 895–898. doi:10.1130/G25356A.1.

Baadsgaard, H., Folinsbee, R.E., and Lipson, J. 1961. Potassium-argon dates of biotites from Cordilleran granites. Geological Society of America Bulletin, **72**: 689–702. doi:10.1130/0016-7606(1961)72[689:PDOBFC]2.0.CO;2.

Bacon, C.R., and Lanphere, M.A. 2006. Eruptive history and geochronology of Mount Mazama and the Crater Lake region, Oregon. Geological Society of America Bulletin, **118**: 1331–1359. doi:10.1130/B25906.1.

Beck, M.E., and Burr, C.D. 1979. Paleomagnetism and tectonic significance of the Goble Volcanic Series, southwestern Washington. Geology, **7**: 175–179. doi:10.1130/0091-7613(1979)7<175:PATSOT>2.0.CO;2.

Berman, R.G., and Armstrong, R.L. 1980. Geology of the Coquihalla Volcanic Complex, southwestern British Columbia. Canadian Journal of Earth Sciences, **17**: 985–995. doi:10.1139/e80-099.

Botros, M., and Johnson, H.P. 1988. Tectonic evolution of the Explorer-Northern Juan de Fuca Region from 8 Ma to the present. Journal of Geophysical Research: Solid Earth, **93**(B9): 10421–10437. doi:10.1029/JB093iB09p10421.

Breitsprecher, K., Thorkelson, D.J., Groome, W.G., and Dostal, J. 2003. Geochemical confirmation of the Kula-Farallon slab window beneath the Pacific Northwest in Eocene time. Geology, **31**: 351–354. doi:10.1130/0091-7613(2003)031<0351:GCOTKF>2.0.CO;2.

Brown, E.H. 2012. Obducted nappe sequence in the San Juan Islands – northwest Cascades thrust system, Washington and British Columbia. Canadian Journal of Earth Sciences, **49**: 796–817. doi:10.1139/e2012-026.

Brown, E.H., and Gehrels, G.E. 2007. Detrital zircon constraints on terrane ages and affinities and timing of orogenic events in the San Juan Islands and North Cascades, Washington. Canadian Journal of Earth Sciences, **44**: 1375–1396. doi:10.1139/e07-040.

Brown, E.H., Gehrels, G.E., and Valencia, V.A. 2010. Chilliwack composite terrane in northwest Washington: Neoproterozoic-Silurian passive margin basement, Ordovician-Silurian arc inception. Canadian Journal of Earth Sciences, **47**: 1347–1366. doi:10.1139/E10-047.

Campbell, M.E., Russell, J.K., and Porritt, L.A. 2013. Thermomechanical milling of accessory lithics in volcanic conduits. Earth and Planetary Science Letters, **377**: 276–286. doi:10.1016/j.epsl.2013.07.008.

Cassidy, J.F., Ellis, R.M., Karavas, C., and Rogers, G.C. 1998. The northern limit of the subducted Juan de Fuca plate system. Journal of Geophysical Research: Solid Earth, **103**(B11): 26949–26961. doi:10.1029/98JB02140.

Clynne, M.A., Calvert, A.T., Wolfe, E.W., Evarts, R.C., Fleck, R.J., and Lanphere, M.A. 2008. Magmatic conditions and processes in the storage zone of the 2004–2006 Mount St. Helens dacite. *In* A volcano rekindled; the renewed eruption of Mount St. Helens, 2004–2006, Chapter 28. *Edited by* D.R. Sherrod, W.E. Scott, and P.H. Stauffer. U.S. Geological Survey, Professional Paper 1750, pp. 593–627.

Coish, R.A., and Journeay, J.M. 1992. The Crevasse Crag Volcanic Complex, southwestern British Columbia: structural control on the geochemistry of arc magmas. *In* Current Research, Part A; Cordillera and Pacific Margin. Geological Survey of Canada, Paper 92-IA, pp. 95–103.

Corfu, F., Hanchar, J.M., Hoskin, P.W.O., and Kinny, P. 2003. Atlas of zircon textures. *In* Zircon; Reviews in Mineralogy and Geochemistry. *Edited by* J.M. Hanchar and P.W.O. Hoskin. Mineralogical Society of America, Washington, D.C., Vol. 53, pp. 468–500. doi:10.2113/0530469.

Dalrymple, G.B. 1979. Critical tables for the conversion of K-Ar ages from old to new constants: Geology, **7**: 558–560. doi:10.1130/0091-7613(1979)7<558:CTFCOK>2.0.CO;2.

De Silva, S.L., Riggs, N.R., and Barth, A.P. 2015. Quickening the Pulse: Fractal Tempos in Continental Arc Magmatism. Elements, **11**: 113–118. doi:10.2113/gselements.11.2.113.

Dickinson, W.R. 2004. Evolution of the North American Cordillera. Annual Reviews in Earth and Planetary Sciences, **32**: 13–45. doi:10.1146/annurev.earth.32.101802.120257.

du Bray, E.A., and John, D.A. 2011. Petrologic, tectonic, and metallogenic evolution of the Ancestral Cascades magmatic arc, Washington, Oregon, and northern California. Geosphere, **7**(5): 1102–1133. doi:10.1130/GES00669.1.

du Bray, E.A., Bacon, C.R., John, D.A., Wooden, J.L., and Mazdab, F.K. 2011. Episodic intrusion, internal differentiation, and hydrothermal alteration of the Miocene Tatoosh intrusive suite south of Mount Rainier, Washington. Geological Society of America Bulletin, **123**(3–4): 534–561. doi:10.1130/B30095.1.

du Bray, E.A., John, D.A., and Cousens, B.L. 2014. Petrologic, tectonic, and metallogenic evolution of the southern segment of the ancestral Cascades magmatic arc, California and Nevada. Geosphere, **10**(1): 1–39. doi:10.1130/GES00944.1.

Duncan, R.A., and Kulm, L.D. 1989. Plate tectonic evolution of the Cascades arc-subduction complex. *In* Geology of North America; the eastern Pacific Ocean and Hawaii. *Edited by* E.L. Winterer, et al. Geological Society of America, Boulder, Colorado, vol. N, pp. 413–438.

Engels, J.C., Tabor, R.W., Miller, F.K., and Obradovich, J.D. 1976. Summary of K-Ar, Rb-Sr, U-Pb, Pbα, and fission-track ages of rocks from Washington State prior to 1975 (exclusive of Columbia Plateau basalts). U.S. Geological Survey, Miscellaneous Field Studies Map MF-710.

Evarts, R.C., Ashley, R.P., and Smith, J.G. 1987. Geology of the Mount St. Helens area: Record of discontinuous volcanic and plutonic activity in the Cascade arc of southern Washington. Journal of Geophysical Research, **92**(B10): 10155–10169. doi:10.1029/JB092iB10p10155.

Fleck, R.J., Hagstrum, J.T., Calvert, A.T., Evarts, R.C., and Conrey, R.M. 2014. $^{40}Ar/^{39}Ar$ geochronology, paleomagnetism, and evolution of the Boring volcanic field, Oregon and Washington, USA. Geosphere, **10**(6): 1283–1314. doi:10.1130/GES00985.1.

Green, N.L., Armstrong, R.L., Harakal, J.E., Souther, J.G., and Read, P.B. 1988. Eruptive history and K-Ar geochronology of the late Cenozoic Garibaldi volcanic belt, southwestern British Columbia. Geological Society of America Bulletin, **100**: 563–579. doi:10.1130/0016-7606(1988)100<0563:EHAKAG>2.3.CO;2.

Hildreth, W.H. 2007. Quaternary magmatism in the Cascades; geologic perspectives. United States Geological Survey Professional Paper 1744, 125 p.

Hildreth, W., and Fierstein, J. 2015. Geologic map of the Simcoe Mountains volcanic field, main central segment, Yakama Nation, Washington. United States Geological Survey Scientific Investigations, Map 3315, 76 p.

Hildreth, W., and Lanphere, M.A. 1994. Potassium-argon geochronology of a basalt-andesite-dacite arc system: The Mount Adams volcanic field, Cascade Range of southern Washington. Geological Society of America Bulletin, **106**: 1413–1429. doi:10.1130/0016-7606(1994)106<1413:PAGOAB>2.3.CO;2.

Hildreth, W., Fierstein, J., and Lanphere, M. 2003. Eruptive history and geochronology of the Mount Baker volcanic field, Washington. Geological Society of America Bulletin, **115**: 729–764. doi:10.1130/0016-7606(2003)115<0729:EHAGOT>2.0.CO;2.

Hildreth, W., Lanphere, M.A., Champion, D.E., and Fierstein, J. 2004. Rhyodacites of Kulshan caldera, North Cascades of Washington: Postcaldera lavas that span the Jaramillo. Journal of Volcanology and Geothermal Research, **130**(3–4): 227–264. doi:10.1016/S0377-0273(03)00290-7.

Jackson, S.E., Pearson, N.J., Griffin, W.L., and Belousova, E.A. 2004. The application of laser ablation-inductively coupled plasma-mass spectrometry to *in situ* U–Pb zircon geochronology. Chemical Geology, **211**: 47–69. doi:10.1016/j.chemgeo.2004.06.017.

Jicha, B.R., Johnson, C.M., Hildreth, W., Beard, B.L., Hart, G.L., Shirey, S.B., and Singer, B.S. 2009. Discriminating assimilants and decoupling deep- vs. shallow-level crystal records at Mount Adams using ^{238}U-^{230}Th disequilibria and Os isotopes. Earth and Planetary Science Letters, **277**: 38–49. doi:10.1016/j.epsl.2008.09.035.

Journeay, J.M., and Friedman, R.M. 1993. The Coast Belt thrust system: Evidence of late Cretaceous shortening in southwest British Columbia. Tectonics, **12**: 756–775. doi:10.1029/92TC02773.

Jutzeler, M., McPhie, J., and Allen, S.R. 2014. Facies architecture of a continental, below-wave-base volcaniclastic basin: The Ohanapecosh Formation, Ancestral Cascades arc (Washington, USA). Geological Society of America Bulletin, **126(3/4)**: 352–376. doi:10.1130/B30763.1.

Kirsch, M., Paterson, S.R., Wobbe, F., Martinez-Ardila, A.M., Clausen, B.L., and Alasino, P.H. 2016. Temporal histories of Cordilleran continental arcs: Testing models for magmatic episodicity. American Mineralogist, **101**: 2133–2154. doi:10.2138/am-2016-5718.

Levander, A., and Miller, M.S. 2012. Evolutionary aspects of lithosphere discontinuity structure in the western U.S. Geochemistry, Geophysics, Geosystems, **13**: Q0AK07. doi:10.1029/2012GC00405.

Lopez-Sanchez, M.A., Aleinikoff, J.N., Marcos, A., Martinez, F.J., and Llana Funez, S. 2016, An example of low-Th/U zircon overgrowths of magmatic origin in a late orogenic Variscan intrusion: the San Ciprián massif (NW Spain). Journal of the Geological Society, **173**: 282–291. doi:10.1144/jgs2015-071.

Ludwig, K.R. 2001. User's manual for Isoplot/Ex Version 2.49, a geochronological toolkit for Microsoft Excel. Berkeley Geochronological Center, Special Publication 1a, Berkeley, USA, 55 p.

Lux, D.R. 1981. Geochronology, geochemistry and petrogenesis of basaltic rocks from the Western Cascades, Oregon. Ph.D. thesis, The Ohio State University, Columbus, 171 p.

Madsen, J.K., Thorkelson, D.J., Friedman, R.M., and Marshall, D.D. 2006. Cenozoic to Recent plate configurations in the Pacific Basin: Ridge subduction and slab window magmatism in western North America. Geosphere, **2**(1): 11–34. doi:10.1130/GES00020.1.

Mahoney, J.B., Friedman, R.M., and McKinley, S.D. 1995. Evolution of a Middle Jurassic volcanic arc: stratigraphic, isotopic, and geochemical characteristics

of the Harrison Lake Formation, southwestern British Columbia. Canadian Journal of Earth Sciences, **32**: 1759–1776. doi:10.1139/e95-137.

Mathews, W.H., Berman, R.G., and Harakal, J.E. 1981. Mid-Tertiary volcanic rocks of the Cascade Mountains, southwestern British Columbia, ages and correlations. Canadian Journal of Earth Sciences, **18**: 662–664. doi:10.1139/e81-059.

Mattinson, J.M. 1977. Emplacement history of the Tatoosh volcanic-plutonic complex, Washington: Ages of zircons. Geological Society of America Bulletin, **88**(10): 1509–1514. doi:10.1130/0016-7606(1977)88<1509:EHOTTV>2.0.CO;2.

McBirney, A.R. 1978. Volcanic evolution of the Cascade Range. Annual Review of Earth and Planetary Sciences, **6**: 437–456. doi:10.1146/annurev.ea.06.050178.002253.

McCaffrey, R., Qamar, A.I., King, R.W., Wells, R.E., Ning, Z., Williams, C.A., et al. 2007. Fault locking, block rotation, and crustal deformation in the Pacific Northwest: Geophysical Journal International, **169**: 1315–1340. doi:10.1111/j.1365-246X.2007.03371.x.

McCaffrey, R., King, R.W., Payne, S.J., and Lancaster, M. 2013. Active tectonics of northwestern US inferred from GPS-derived surface velocities: Journal of Geophysical Research, **118**: 709–723. doi:10.1029/2012JB009473.

McCrory, P.A., and Wilson, D.S. 2013. A kinematic model for the formation of the Siletz-Crescent forearc terrane by capture of coherent fragments of the Farallon and Resurrection plates. Tectonics, **32**: 718–736. doi:10.1029/2013TC, 10.1002/tect.20045.

McCrory, P.A., Hyndman, R.D., and Blair, J.L. 2014. Relationship between the Cascadia fore-arc mantle wedge, nonvolcanic tremor, and the downdip limit of seismogenic rupture. Geochemistry, Geophysics, Geosystems, **15**(4): 1071–1095. doi:10.1002/2013GC005144.

Miller, K.C., Keller, G.R., Gridley, J.M., Luetgert, J.H., Mooney, W.D., and Thybo, H. 1997. Crustal structure along the west flank of the Cascades, western Washington. Journal of Geophysical Research: Solid Earth, **102**(B8): 17857–17873. doi:10.1029/97JB00882.

Miller, R.B., Paterson, S.R., and Matzel, J.P. 2009. Plutonism at different crustal levels: Insights from the ~5-40 km (paleodepth) North Cascades crustal section, Washington. *In* Crustal cross sections from the western North American Cordillera and elsewhere: Implications for tectonic and petrologic processes. *Edited by* R.B. Miller and A.W. Snoke. Geological Society of America, Special Paper **456**: 125–149. doi:10.1130/2009.2456(05).

Monger, J.W.H. 1989. Geology of Hope and Ashcroft map areas. Geological Survey of Canada, Maps 41-1989, 42-1989, scale 1:250,000.

Monger, J.W.H., and Journeay, J.M. 1994. Guide to the geology and tectonic evolution of the southern Coast Mountains. Geological Survey of Canada, Open File 2490, 77 p.

Monger, J.W.H., and Price, R.A. 2000. A transect of the southern Canadian Cordillera from Vancouver to Calgary. Geological Survey of Canada, Open File 3902, 170 p.

Monger, J.W.H., Price, R.A., and Tempelman-Kluit, D.J. 1982. Tectonic accretion and the origin of the two major metamorphic and plutonic welts in the Canadian Cordillera. Geology, **10**: 70–75. doi:10.1130/0091-7613(1982)10<70:TAATOO>2.0.CO;2.

Muffler, L.J.P., Clynne, M.A., Calvert, A.T., and Champion, D.E. 2011. Diverse, discrete, mantle-derived batches of basalt erupted along a short normal fault zone: The Poison Lake chain, southernmost Cascades. Geological Society of America Bulletin, **123**(11–12): 2177–2200. doi:10.1130/B30370.1.

Mullen, E.K. 2011. Petrology and geochemistry of the Mount Baker volcanic field: Constraints on source regions and terrane boundaries, and comparison with other Cascade Arc volcanic centers. Ph.D. dissertation, University of Washington, Seattle, 388 p.

Mullen, E.K., and McCallum, I.S. 2014. Origin of basalts in a hot subduction setting: petrological and geochemical insights from Mt. Baker, northern Cascade arc. Journal of Petrology, **55**(2): 241–281. doi:10.1093/petrology/egt064.

Mullen, E.K., and Weis, D. 2013. Sr-Nd-Hf-Pb isotope and trace element evidence for the origin of alkalic basalts in the Garibaldi Belt, northern Cascade arc. Geochemistry, Geophysics, Geosystems, **14**(8): 3126–3155. doi:10.1002/ggge.20191.

Mullen, E.K., and Weis, D. 2015. Evidence for trench-parallel mantle flow in the northern Cascade Arc from basalt geochemistry. Earth and Planetary Science Letters, **414**: 100–107. doi:10.1016/j.epsl.2015.01.010.

Mullen, E.K., Weis, D., Marsh, N.B., and Martindale, M. 2017. Primitive arc magma diversity: New geochemical insights in the Cascade Arc. Chemical Geology, **448**: 43–70. doi:10.1016/j.chemgeo.2016.11.006.

Müller, W., Shelley, M., Miller, P., and Broude, S. 2009. Initial performance metrics of a new custom-designed ArF excimer LA-ICPMS system coupled to a two-volume laser-ablation cell. Journal of Analytical Atomic Spectrometry, **24**: 209–214. doi:10.1039/B805995K.

Nixon, G.T., and Orr, A.J. 2007. Recent revisions to the Early Mesozoic stratigraphy of Northern Vancouver Island (NTS 102I; 092L) and metallogenic implications, British Columbia. *In* Geological Fieldwork 2006. *Edited by* B. Grant. British Columbia, Ministry of Energy, Mines and Petroleum Resources, Paper 2007-1, pp. 163–177.

Paquette, J.L., Piro, J.L., Devidal, J.L., Bosse, V., and Didier, A. 2014. Sensitivity enhancement in LA-ICP-MS by N_2 addition to carrier gas: application to radiometric dating of U-Th-bearing minerals. Agilent ICP-MS Journal, **58**: 4–5.

Paterson, S.R., and Ducea, M.N. 2015. Arc magmatic tempos: Gathering the evidence. Elements, **11**: 91–98. doi:10.2113/gselements.11.2.91.

Phillips, W.M. 1987. Geologic map of the Mount St. Helens quadrangle, Washington and Oregon. Washington Division of Geology and Earth Resources, Open File Report 87-4, 48 p., scale 1:100,000.

Priest, G.R. 1990 Volcanic and tectonic evolution of the Cascade Volcanic Arc, Central Oregon. Journal of Geophysical Research, **95**: 19583–19599. doi:10.1029/JB095iB12p19583.

Ray, G.E. 1986. Gold associated with a regionally developed mid-Tertiary plutonic event in the Harrison Lake area, southwestern British Columbia (92G/9; 92H/3,4,5,6,12). *In* British Columbia Ministry of Energy, Mines and Petroleum Resources, Geological Fieldwork 1985, Paper 1986-1, pp. 95–97.

Ray, G.E., and Coombes, S. 1985. Harrison Lake Project (92H/5,12; 92G/9,16). *In* British Columbia Ministry of Energy, Mines and Petroleum Resources, Geological Fieldwork 1984, Paper 1985-1, pp. 120–132.

Reiners, P.W., Hammond, P.E., McKenna, J.M., and Duncan, R.A. 2000, Young basalts of the central Washington Cascades, flux melting of the mantle, and trace element signatures of primary arc magmas. Contributions to Mineralogy and Petrology, **138**: 249–264. doi:10.1007/s004100050561.

Reiners, P.W., Ehlers, T.A., Garver, J.I., Mitchell, S.G., Montgomery, D.R., Vance, J.A., and Nicolescu, S. 2002. Late Miocene exhumation and uplift of the Washington Cascade Range. Geology, **30**: 767–770. doi:10.1130/0091-7613(2002)030<0767:LMEAUO>2.0.CO;2.

Richards, T.A., and McTaggart, K.C. 1976. Granitic rocks of the southern Coast Plutonic Complex and northern Cascades of British Columbia. Geological Society of America Bulletin, **87**(6): 935–953. doi:10.1130/0016-7606(1976)87<935:GROTSC>2.0.CO;2.

Riddihough, R. 1984. Recent movements of the Juan de Fuca plate system. Journal of Geophysical Research: Solid Earth, **89**: 6980–6994. doi:10.1029/JB089iB08p06980.

Rohr, K.M.M. 2015, Plate boundary adjustments of the southernmost Queen Charlotte fault. Bulletin of the Seismological Society of America, **105**: 1–14. doi:10.1785/0120140162.

Rohr, K.M.M., and Tryon, A.J. 2010. Pacific-North America plate boundary reorganization in response to a change in relative plate motion: Offshore Canada. Geochemistry Geophysics Geosystems, **11**: Q06007. doi:10.1029/2009GC003019.

Schärer, U. 1984. The effect of initial Th-230 disequilibrium on young U-Pb Ages: the Makalu Case, Himalaya. Earth Planet Science Letters, **67**: 191–204. doi:10.1016/0012-821X(84)90114-6.

Schasse, H.W. 1987. Geologic map of the Mount Rainier quadrangle, Washington: Washington Division of Geology and Earth Resources, Open-File Report 87-16, 43 p., scale 1:100,000.

Schellart, W.P., Stegman, D.R., Farrington, R.J., Freeman, J., and Moresi, L. 2010. Cenozoic tectonics of western North America controlled by evolving width of Farallon slab. Science, **329**: 316–319.

Schmidt, M.E., and Grunder, A.L. 2009. The evolution of North Sister: A volcano shaped by extension and ice in the central Oregon Cascade Arc. GSA Bulletin, **121**(5–6): 643–662. doi:10.1130/B26442.1.

Sherrod, D.R., and Smith, J.G. 2000. Geologic map of upper Eocene to Holocene volcanic and related rocks of the Cascade Range, Oregon: U.S. Geological Survey Miscellaneous Investigations Series Map I-2569, scale 1:500,000, 17 p.

Souther, J.G. 1977. Volcanism and tectonic environments in the Canadian Cordillera – A second look. *Edited by* W.R.A. Baragar, et al. *In* Volcanic Regimes in Canada: Geological Association of Canada Special Paper, Vol. 16, pp. 3–24.

Souther, J.G., and Yorath, C.J. 1991. Neogene assemblages, Chapter 10. *In* Geology of the Cordilleran Orogen in Canada. *Edited by* H. Gabrielse and C.J. Yorath. Geological Survey of Canada, Geology of Canada, No. 4, pp. 373–401.

Stevens, R.D., Delabio, R.N., and Lachance, G. 1982. Age determinations and geologic studies, K-Ar isotopic ages. Report 15: Geological Survey of Canada Paper 81-2, 56 p.

Tabor, R.W., and Crowder, D.F. 1969. On batholiths and volcanoes; intrusion and eruption of late Cenozoic magmas in the Glacier Peak area, North Cascades, Washington: U.S. Geological Survey Professional Paper 604, 67 p.

Tabor, R.W., Frizzell, V.A., Jr., Booth, D.B., Waitt, R.B., Whetten, J.T., and Zartman, R.E. 1993. Geologic map of the Skykomish 60-minute by 30-minute quadrangle, Washington: U.S. Geological Survey Geologic Investigations Series Map I-1963, scale 1:100,000, 42 p.

Tabor, R.W., Frizzell, V.A., Jr., Booth, D.B., and Waitt, R.B. 2000, Geologic map of the Snoqualmie Pass 30- 32 × 60-minute quadrangle, Washington: U.S. Geological Survey Geologic Investigations Series Map I-2538, scale, 1:100,000, 57 p.

Tabor, R.W., Booth, D.B., Vance, J.A., and Ford, A.B. 2002. Geologic map of the Sauk River 30- × 60-minute quadrangle, U.S. Geological Survey Miscellaneous Investigations Map I-2592, scale 1:100,000.

Tabor, R.W., Haugerud, R.A., Hildreth, W., and Brown, E.H. 2003. Geologic map of the Mount Baker 30 × 60 minute quadrangle, Washington: U.S. Geological Survey Map I-2660, scale 1:100,000.

Tepper, J.H. 1991. Petrology of mafic plutons and their role in granitoid genesis, Chilliwack batholith, North Cascades, Washington. Ph.D. Dissertation, University of Washington, Seattle, 307 p.

Tepper, J.H. 1996. Petrology of mafic plutons associated with calc-alkaline granitoids, Chilliwack batholith, North Cascades, Washington. Journal of Petrology, **37**(6): 1409–1436. doi:10.1093/petrology/37.6.1409.

Tepper, J.H. 2002. Correlation of chemical trends in Cascade Arc granitoids with Tertiary plate motions. Geological Society of America, Abstracts with Programs, **34**(5): 17.

Tepper, J.H., and Hildreth, W. 2004, The plutonic-volcanic connection in the Cascade Arc; insights from the Mount Baker-Chilliwack area, WA. Geological Society of America, Abstracts with Programs, **36**(5): 223.

Tepper, J.H., Nelson, B. K, Bergantz, G.W., and Irving, A.J. 1993, Petrology of the Chilliwack batholith, North Cascades, Washington: generation of calc-alkaline granitoids by melting of mafic lower crust with variable water fugacity. Contributions to Mineralogy and Petrology, **113**: 333–351.

Tera, F., and Wasserburg, G.J. 1972. U-Th-Pb systematics in three Apollo 14 basalts and the problem of initial Pb in lunar rocks. Earth and Planetary Science Letters, **14**: 281–304. doi:10.1016/0012-821X(72)90128-8.

Tucker, D., Hildreth, W., Ullrich, T., and Friedman, R. 2007. Geology and complex collapse mechanisms of the 3.72 Ma Hannegan caldera, North Cascades, Washington, USA. Geological Society of America Bulletin, **119**: 329–342. doi: 10.1130/B25904.1.

van Achterbergh, E., Ryan, C.G., Jackson, S.E., and Griffin, W.L. 2001. Data reduction software for LA-ICP-MS. *In* Laser ablation-ICPMS in the earth science. *Edited by* P. Sylvester. Mineralogical Association of Canada, Vol. 29, pp. 239–243.

Verplanck, E.P., and Duncan, R.A. 1987. Temporal variations in plate convergence and eruption rates in the western Cascades, Oregon. Tectonics, **6**: 197–209. doi:10.1029/TC006i002p00197.

Wanless, R.K., Stevens, A.O., Lachance, G.R., and Delabio, R.N. 1978. Age determinations and geologic studies, K-Ar isotopic ages, Report 13: Geological Survey of Canada Paper 77-2, 60 p.

Wells, R.E., and Heller, P.L. 1988. The relative contribution of accretion, shear, and extension to Cenozoic tectonic rotation in the Pacific Northwest. Bull. Geol. Soc. America **100**: 325–338

Wells, R.E., and McCaffrey, R. 2013. Steady rotation of the Cascade arc. Geology, **41**: 1027–1030. doi:10.1130/G34514.1.

Wells, R., Bukry, D., Friedman, R., Pyle, D., Duncan, R., Haeussler, P., and Wooden, J. 2014. Geologic history of Siletzia, a large igneous province in the Oregon and Washington Coast Range: correlation to the geomagnetic polarity time scale and implications for a long-lived Yellowstone hotspot. Geosphere, **10**: 692–719. doi:10.1130/GES01018.1.

Westgate, J.A., Easterbrook, D.J., Naeser, N.D., and Carson, R.J. 1987. Lake Tapps tephra: An early Pleistocene stratigraphic marker in the Puget Lowland, Washington. Quaternary Research, **28**: 340–355.

Wiedenbeck, M., Allé, P., Corfu, F., Griffin, W.L., Meier, M., Oberli, F, et al. 1995. Three natural zircon standards for U-Th-Pb, Lu-Hf, trace element and REE analyses. Geostandards and Geoanalytical Research, **19**(1): 1–23. doi:10.1111/j.1751-908X.1995.tb00147.x.

Wilson, D.S. 1988. Tectonic history of the Juan de Fuca ridge over the last 40 million years. Journal of Geophysical Research, **93**: 11863–11876. doi:10.1029/JB093iB10p11863.

Woodsworth, G.J. 1977. Pemberton (92J) map area. Geological Survey of Canada Open File Report 482, scale 1:250,000.

Woodsworth, G.J., Anderson, R.G., and Armstrong, R.L. 1991. Plutonic regimes, Chapter 15. *In* Geology of the Cordilleran Orogen in Canada. *Edited by* H. Gabrielse and C.J. Yorath. Geological Survey of Canada, Geology of Canada, No. 4, pp. 491–531.

Wright, N.M., Seton, M., Williams, S.E., and Müller, R.D. 2016. The Late Cretaceous to recent tectonic history of the Pacific Ocean basin. Earth Science Reviews, **154**: 138–173. doi:10.1016/j.earscirev.2015.11.015.

Zelt, B.C., Ellis, R.M., and Clowes, R.M. 1993. Crustal velocity structure in the eastern Insular and southernmost Coast Belts, Canadian Cordillera. Canadian Journal of Earth Science, **30**: 1014–1027. doi:10.1139/e93-085.